Dimensional artefacts to achieve metrological traceability in advanced manufacturing

CIRP Annals - Manufacturing Technology

Dimensional artefacts to achieve metrological traceability in advanced manufacturing

--Manuscript Draft--

Manuscript Number:	2020-P-KeynoteR2
Article Type:	STC P
Keywords:	Manufacturing metrology; Traceability; Dimensional artefacts
Corresponding Author:	Simone Carmignato University of Padova Vicenza, ITALY
First Author:	Simone Carmignato
Order of Authors:	Simone Carmignato
	Leonardo De Chiffre
	Harald Bosse
	Richard Leach
	Alessandro Balsamo
	Tyler Estler
Abstract:	Dimensional measurements play a central role in enabling advanced manufacturing technologies, enhancing the quality of products and increasing productivity. This role becomes even more important in the context of Industry 4.0, where reliable and accurate digital models of products, processes and production systems are needed. To establish the traceability chain that links measurements in production to the length unit, dimensional artefacts – ranging from measurement standards to calibrated workpieces – are fundamental. The paper examines dimensional artefacts, discussing their characteristics, availability and role in supporting production by establishing metrological traceability, and provides guidelines for their selection, use and development

Contents lists available at SciVerse ScienceDirect

CIRP Annals Manufacturing Technology

Journal homepage: www.elsevier.com/locate/cirp

Dimensional artefacts to achieve metrological traceability in advanced manufacturing

S. Carmignato[1] (2), L. De Chiffre[2] (1), H. Bosse[3] (3), R. K. Leach[4] (2), A. Balsamo[5] (1), W. T. Estler[6] (1)

[1] *University of Padova, Italy*
[2] *Technical University of Denmark, Denmark*
[3] *Physikalisch-Technische Bundesanstalt (PTB), Germany*
[4] *University of Nottingham, United Kingdom*
[5] *Istituto Nazionale di Ricerca Metrologica (INRiM), Italy*
[6] *National Institute of Standards and Technology (NIST), United States*

Dimensional measurements play a central role in enabling advanced manufacturing technologies, enhancing the quality of products and increasing productivity. This role becomes even more important in the context of Industry 4.0, where reliable and accurate digital models of products, processes and production systems are needed. To establish the traceability chain that links measurements in production to the length unit, dimensional artefacts – ranging from measurement standards to calibrated workpieces – are fundamental. The paper examines dimensional artefacts, discussing their characteristics, availability and role in supporting production by establishing metrological traceability, and provides guidelines for their selection, use and development.

Keywords: Manufacturing metrology, Traceability, Dimensional artefacts

1. Introduction

The importance of dimensional metrology as a fundamental tool for enabling advanced technologies and adding value in manufacturing is clearly documented in a previous CIRP keynote paper by Kunzmann et al. [179] (see also [250] and [252]). In order to address the constantly increasing needs in advanced manufacturing, a common trend is that, when possible, measurements are integrated directly into production, so that process control and tolerance verification can take place fast enough to allow corrections of the manufacturing processes [104]. This trend is even more evident in connection with Industry 4.0 [210], where measurement data from several sensors, including dimensional data, are intended to be used for monitoring the whole manufacturing process and constantly adjusting the process parameters, involving the creation and use of digital twins [192]. The reliability of process corrections, including those through the application of digital models, will depend highly on the accuracy and traceability of the measurement data that are fed into the correction models. More generally, traceability of measurements is a prerequisite for obtaining reliable measurement data to control manufacturing processes and assure the quality of products [163], as well as for the comparability of the properties of components in a global manufacturing environment (see Sect. 2). Therefore, manufacturing metrology should not be seen merely as a supplier of data for advanced manufacturing. Manufacturing metrology is rather the "pacemaker" in the concept of Industry 4.0 [139], due to its role in cyber-physical systems, linking together the "digital world" and the "physical world" (see Figure 1). Advanced manufacturing processes, products and measuring systems can be enabled when they can be modelled and controlled effectively and accurately, which is possible only when based on traceable measurement data.

Establishment of traceability requires evaluation of measurement uncertainty and realisation of an unbroken chain of calibrations to relate a measurement result to a reference [163]. Figure 2 illustrates a typical transfer of traceability in production using calibrated workpieces (or calibrated master parts). Depending on the manufacturing process and the production requirements, establishment of the required reference can become an arduous task, as is often the case, for example, in connection with additive manufacturing (AM), where the parts may contain

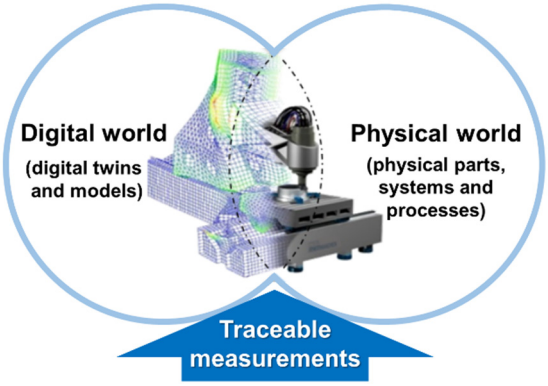

Figure 1. Traceable measurements are fundamental for linking together digital and physical worlds in cyber-physical systems (adapted from [139]).

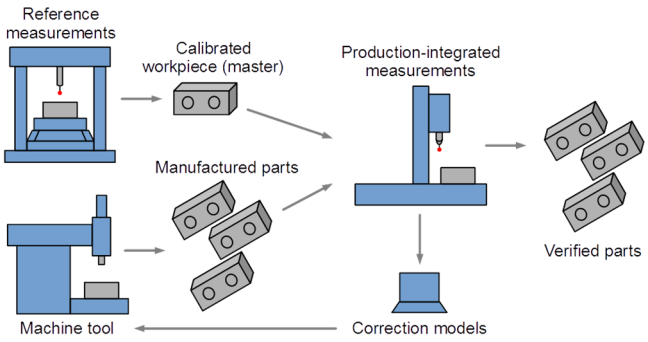

Figure 2. Example of traceability establishment for production-integrated coordinate measurements by implementation of the substitution method, using calibrated workpieces according to the ISO 15530-3 [152], and use of traceable measurement results for controlling a manufacturing process.

hidden and internal features that are difficult to emulate with a calibrated physical object [187]. Therefore, numerous solutions have been developed to achieve traceability using different types of artefacts, ranging from well-established objects with simple geometry, such as gauge blocks, to complex artefacts for specific applications, such as assemblies with calibrated internal features (see Sect. 3).

Inspired by the CIRP keynotes [70], [91] and [289], this paper gives an overview of "dimensional artefacts", in the sense of "material measures" that can be used to establish traceability of dimensional measurements. A "material measure" is defined in the International Vocabulary of Metrology (VIM) [163] as a *"measuring instrument reproducing or supplying, in a permanent manner during its use, quantities of one or more given kinds, each with an assigned quantity value"*. In the paper, the term "dimensional artefact" (often shortened to "artefact" below) is preferred to the term "dimensional material measure" because of its simplicity and wider use in manufacturing metrology. Dimensional artefacts range from measurement standards (defined in the VIM as a *"realization of the definition of a given quantity, with stated quantity value and associated measurement uncertainty, used as a reference"*) to calibrated workpieces (including workpiece-like artefacts and master workpieces).

The paper is intended to serve as a guideline for users in manufacturing industry and research, for the selection, use, and development of dimensional artefacts to support production by establishing the traceability of measurements. Since the area of metrological traceability is very broad, the scope of the paper is restricted as follows: (1) the paper covers artefacts but does not cover indicating measuring instruments (i.e. it covers "passive" objects, but not "active" measuring instruments); (2) the paper considers only artefacts used for achieving traceability, rather than objects used for tolerance verification (such as limit gauges); (3) in addition, the focus of the paper is on dimensional artefacts applied in manufacturing metrology and not in other fields.

The paper is organised as follows. Section 2 clarifies the role of dimensional artefacts in supporting production by establishing metrological traceability. Section 3 presents the main state-of-the-art dimensional artefacts, covering linear dimensions (Sect. 3.1), form and surface texture (Sect. 3.2), complex geometry (Sect. 3.3), and angle (Sect. 3.4). Section 4 discusses the availability of dimensional artefacts, while Section 5 provides guidelines for their development. Finally, general conclusions and an outlook are reported in Section 6.

2. Supporting production by traceability using dimensional artefacts

The traceability concept has been discussed in [179] as a necessary foundation for manufacturing metrology, showing that traceable measurements generate value in production, and provide knowledge that is then used as a basis for decisions and actions. It is noted in the VIM that metrological traceability requires an established calibration hierarchy. The documented unbroken chain of calibrations is often visualised by the so-called calibration pyramid (see Figure 3), with the International System of Units (SI) located at the top, followed by calibrations performed at national metrology institutes (NMIs), accredited calibration laboratories, and in-plant calibration laboratories, and finally by the manufacturing measurements and the manufacturing process control based on calibrated sensors, artefacts and measuring instruments, ensuring the traceability and comparability of measurement results. Usually the measurement uncertainty and the number of calibrated measuring instruments or measurement standards are increased at every step going down the calibration pyramid. The calibration and measurement capabilities (CMCs) of the NMIs are listed in the so-called Key Comparison Data Base (KCDB) of the International Bureau of Weights and Measures (*Bureau International des Poids et Mesures* – BIPM) [29]. The requirements for testing and calibration laboratories, including the NMIs, are harmonised worldwide and described in the international standard ISO/IEC 17025 [156]. This international standard requires that calibrations and measurements made by the laboratory are traceable to the SI. Following a discussion originally initiated by the National Institute of Standards and Technology (NIST) [273], the American Society of Mechanical Engineers (ASME) published a guideline focussing specifically on the traceability of dimensional measurements [11].

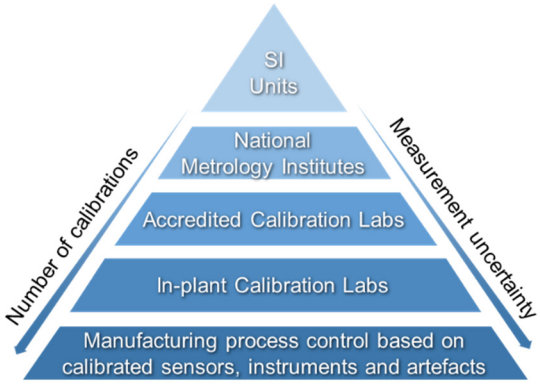

Figure. 3. Calibration pyramid.

In ancient cultures, the development and maintenance of a practical, reliable and accepted system of weights and measures was regarded as a governmental task and the necessary base for all measurements performed in daily life. For example, in ancient Egypt the royal cubit (the length of the Pharaoh's forearm) served as the length reference and wooden copies of it (see Fig. 4-a) were manufactured and maintained by civil servants and distributed for practical length measurements in daily life [38]. These copies or dimensional artefacts were directly traceable to the reference, the royal cubit, and thus guaranteed the comparability and reliability of length measurements performed in ancient Egypt.

For centuries, different length references (see Fig. 4), either end standards, i.e. artefacts with parallel end faces, or line scales, i.e. artefacts with marked graduation lines on their top surface, were used as length references in different states and even different regions, which turned out to be a severe barrier to trade and industrialisation. Driven by the requirements from early industrialisation and associated concepts, such as the interchangeability of parts, the need for a more accurate and robust length reference was identified, which ideally should also be widely adopted in the industrialised nations.

In France, the metric system was established in 1799 based on the *Mètre des Archives*, an end standard made from platinum whose length was defined to be the 1/10 000 000 part of the quarter meridian of the earth, which was assumed as a stable and universal dimension [38]. In 1875, the metre convention was signed by 17 member states which laid ground for the international acceptance of the metric system of units and at the first General Conference of Weights and Measures (CGPM) in 1889, the length of the international metre prototype made from Pt–Ir alloy, or the spacing of its line engravings at ice water temperature, was defined as the length unit traceable to the former *Mètre des Archives*. High-precision length measurements could be performed at relative uncertainty (u_r) levels of 10^{-7} by referring to copies of the international metre prototype, the so-called national metre prototypes (Fig. 4-b) maintained at the NMIs, which were regularly compared or re-calibrated to the international metre prototype maintained at the BIPM.

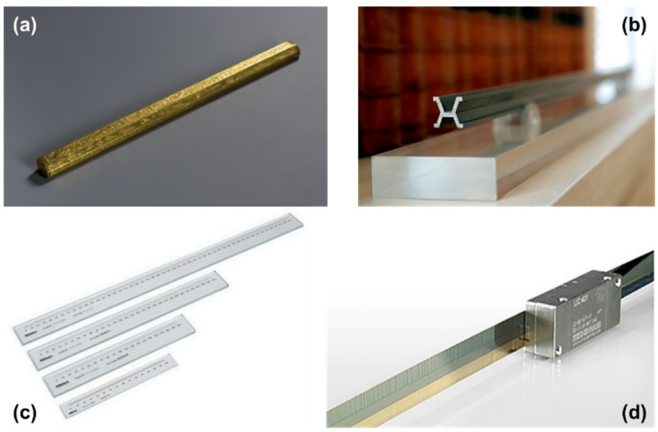

Figure 4. Secular evolution of length artefacts. (a) Gilded wood copy of Egyptian cubit (14th century BC), a combined end standard and linear scale (source: Egyptian Museum of Turin). (b) Copy of international metre prototype in force up to 1960 (source: BIPM). (c) "Passive" line scales (source: Mitutoyo). (d) "Active" line scale, i.e. a linear encoder (source: Heidenhain).

Since 1960, the metrological reference is the SI [31], and the expression *"traceability to the SI"* means *"metrological traceability to a measurement unit of the International System of Units"*. In 1960, the definition of the length unit was changed based on progress in interferometric length measurements. The definition of the length unit was no longer based on a material artefact, the international metre prototype, but on the well-defined vacuum wavelength of the ^{86}Kr spectral lamp [31].

Progress in high-precision laser spectroscopy in the 1970s allowed the measurement of the speed of light in vacuum with comparable uncertainties to interferometric measurements of length based on the wavelength definition. Therefore, in 1983 it was decided to redefine the length unit with a time of flight definition. This definition, which is based on fixing the numerical value of a natural constant, namely the speed of light in vacuum c, is still valid today: *the metre, symbol m, is the SI unit of length. It is defined by taking the fixed numerical value of the speed of light in vacuum c to be 299 792 458 when expressed in the unit m s^{-1}, where the second is defined in terms of the caesium frequency $\Delta\nu_{Cs}$* [31]. This approach to the definition of units also served as a blueprint for the revision of the SI, which was put into force on 20th May 2019, according to Resolution 1, which was approved by the 26th CGPM on 16th November 2018 [31]. Following this resolution, the numerical values of the so-called defining constants of the SI are fixed. The contributions from precision manufacturing and precision dimensional metrology for experiments to determine the numerical values of the above natural constants with the smallest possible uncertainties in the current SI were described in a previous CIRP keynote [38].

While the definition of the unit of length is based on the fixed value of the speed of light in vacuum, both in the old and in the revised SI (only the wording has changed), its realisation using a recommended laser frequency described in the *Mise en Pratique* for the realisation of the metre [30] is only straightforward in a vacuum environment. In an ambient environment, however, the refractive index of air (n_{air}) changes the group velocity of light ($c_{air} < c$, $n_{air} > 1$) depending on the characteristics of air, such as its temperature, pressure and humidity. The realisation of highly accurate length measurements in air, either by time of flight methods over longer distances or by interferometric techniques over distances normally present in manufacturing or laboratory environments, requires accurate determination of the refractive index of air. For example, to achieve a relative target uncertainty of 10^{-7} for laser-based length measurements, an uncertainty of 0.1 K for the determination of air temperature, 37 Pa for the determination of air pressure and approximately 10% for the determination of relative humidity of air is needed [85].

The dependence of interferometric length measurement on the refractive index of air is one of the main reasons for the application of suitable calibrated dimensional artefacts in manufacturing process control today. Well-known examples of one-dimensional (1D) artefacts are end standards, such as gauge blocks, or graduated artefacts, such as line scales (see Sect. 3.1). Moreover, measuring instruments, such as linear or angular encoder systems, are based on line gratings manufactured on the flat surfaces of suitably stable substrates [105]. A systematic analysis and comparison of length measurements based on high precision interferometry on one hand and length encoder systems on the other was published in [178].

The dimensions of materials used in length artefacts or as substrates in encoder systems may vary. The most important influence again is temperature, because the length of the artefact will change with its temperature according to the material specific coefficient of thermal expansion (CTE) [259]. Other influences on the stability of the embodied length values of a dimensional artefact are its dependence on ambient pressure (compressibility), its secular drift [260] and the dependence on its mounting conditions (see Sect. 5).

In all cases where the length of a dimensional artefact is important for its application, the recommended re-calibration periods should take into account prior knowledge about the long-term stability of its material. If, however, an artefact is used primarily for calibration of form deviations of measuring instruments by means of self-calibration techniques [91], the long-term drift of the dimensions of an artefact is only of minor significance for its metrological applicability. One example of such an application is the use of a patterned two-dimensional (2D) artefact, such as a photomask for calibration of the straightness and orthogonality error of a 2D positioning stage only, i.e. without calibrating the length scale of the two positioning axes [294]. Another example is the application of artefacts in angle metrology (polygon, angular graduation), where the overall dimensions may be influenced by drift of the material, but with no detrimental effect on its metrological performance in angle metrology as long as the drift is purely homogenous and isotropic over the material (see Sect. 3.4).

There is an important difference in the traceability chains of dimensional artefacts for unidirectional and bidirectional measurands. Whereas unidirectional measurands are defined between feature edges of the same orientation, bidirectional measurands are defined between opposite feature edges [148], see Figure 5. Examples of unidirectional measurands are distances between equally-oriented features, e.g. between their left edges or between their centre positions. Examples of bidirectional measurands are the width of line features or the diameter of circular features. Artefacts are designed with unidirectional or bidirectional measurands depending on their specific function (see Sect. 5). For example, for verifying the metrological performances of a coordinate measuring system (CMS) when used for bidirectional measurements, bidirectional artefacts are chosen, which may provide significantly different results compared to the performances of the same CMS when used for unidirectional measurements (as demonstrated e.g. in an industrial intercomparison of optical CMSs [52]). The particular metrological challenges for calibration of bidirectional measurands such as diameters of circles or width of line features using optical CMS have been discussed in [173].

As is illustrated schematically in Figure 5, care has to be taken when defining bidirectional measurands, because these depend more strongly on the geometry of feature edges. The sidewall angle of feature edges does not normally influence the measurement results of unidirectional measurands and only slightly increases

their measurement uncertainty. However, for bidirectional measurands of, e.g. the width of a line *w*, the width to be measured has to be clearly defined. This can be done based on either geometrical properties (e.g. bottom linewidth, top linewidth, linewidth at 50% of height) or other properties. In particular, if the structures on the substrate are used in optical applications, e.g. as photomasks in lithographic production of integrated circuits, the optically effective linewidth is of primary interest. Using different measurement methods – e.g. atomic force microscopy (AFM), scanning electron microscopy (SEM), optical microscopy (OM) and scatterometry – in the traceability chain of bidirectional measurands, thus, requires appropriate signal modelling of the respective edge contrasts of the different instruments, based on physical simulations of the interaction of the sample with the measuring probe, to allow the dissemination of the bidirectional measurands with appropriate uncertainty [33], [63], [128].

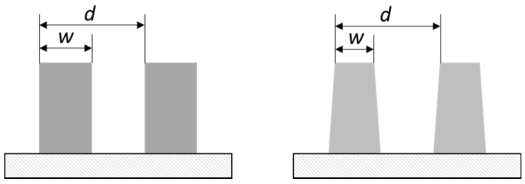

Figure 5. Scheme of unidirectional (*d*) and bidirectional (*w*) measurands defined on line structures showing different edge angles on a substrate: orthogonal edges (left) and sloped edges (right).

The quality of the feature to be measured limits the achievable measurement uncertainty (see Figure 5). Ideally, the smallest measurement uncertainties can be obtained on single crystal materials with atomically defined features for two principle reasons. Firstly, a single crystal material is stable over longer time periods because it does not suffer from long-term relaxation effects in contrast to amorphous, polycrystalline or glass ceramic material [94]. However, silicon has a relatively large CTE of 2.5×10^{-6} K^{-1}; approximately two orders of magnitude larger than the CTE of specialised glass ceramic materials, which are optimised for application in high-precision measuring instruments and machine tools. Secondly, single crystal materials allow the realisation of atomically flat surfaces or feature edges and, thus, offer ideal conditions for the unambiguous definitions of measurands. For example, methods for the preparation of silicon surfaces have recently been developed which allow the realisation of larger atomically flat areas and defined monoatomic steps between the areas, which can be applied as artefacts in surface metrology [165], see Figure 6 for examples from the *Physikalisch-Technische Bundesanstalt* (PTB).

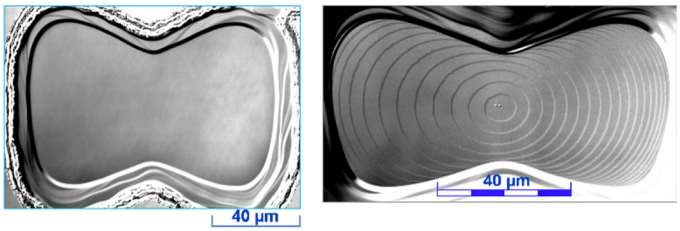

Figure 6. Larger atomically flat areas (left) and areas with monoatomic steps (right), realised on single crystal silicon surfaces (source: PTB).

Another example of the use of single crystalline structures as dimensional artefacts was developed at NIST for linewidth or critical dimension (CD) metrology [60], [77]. Here, an array of line features with widths or CD values of approximately 100 nm or less was prepared from single crystal silicon. One group of these nominally identical line patterns was then prepared by focussed ion beam techniques as a lamella for subsequent imaging in high-resolution transmission electron microscopy (TEM). With this approach, it was possible to determine the width of the silicon lines by counting the number of silicon lattice planes between the left and right boundary of the imaged line feature, using the known lattice parameter value and transferring this value to the other silicon line features, which could be measured by critical dimension AFM techniques, see Figure 7. The silicon lattice parameter d_{220} of natural silicon material was determined by combined optical and X-ray interferometry to be d_{220} = 192.015 5714(32) pm [209]. A similar approach for determination of single crystal silicon linewidth using high-resolution TEM imaging was followed by the PTB [62]. The results of the first comparison on silicon linewidth values at and below 100 nm showed agreement within the expanded measurement uncertainties, which were estimated at 0.7 nm [64].

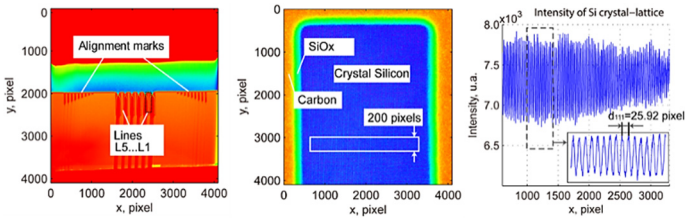

Figure 7. Left: TEM image of silicon line pattern; middle: high-resolution TEM image of one line structure; right: intensity variation of the high-resolution TEM image due to silicon lattice structure (source: PTB).

The use of the single crystal silicon lattice as a secondary realisation of the metre for length measurements at the nanoscale has recently been recommended by the Consultative Committee for Length (CCL) of the International Committee for Weights and Measures (CIPM) [28]. The new version of the *Mise en Pratique* [30] of the metre addresses this recommendation and describes three areas of application, namely: a) realisation of the SI metre using the silicon lattice parameter and X-ray interferometry for nanometre and sub-nanometre scale applications in dimensional nanometrology [286], b) realisation of the SI metre using the silicon lattice and TEM for dimensional nanometrology, and c) realisation of the SI metre using the height of monoatomic steps of crystalline silicon surfaces.

Another type of natural material, which has recently been considered to be used as building blocks and as reference materials for dimensional metrology purposes, is deoxyribonucleic acid (DNA), in particular by means of the DNA origami method [239], [246]. However, the environment of the DNA origami structures has a large impact on their dimensional stability.

Recently, a new type of dimensional artefact based on computer-generated holograms (CGHs) was proposed, e.g. as virtual three-dimensional (3D) calibration artefacts for multi-axis machine tools [227]. The virtual features on the CGH (microstructured fused silica photomask substrate) are measured with a point source of light, e.g. an autostigmatic microscope (ASM). The location of the ball centres in two directions parallel to the plane of the CGH can be read by the ASM with a resolution of less than 1 µm, and to a few micrometres in the third dimension. In the example shown in Figure 8, a ball array CGH was probed by a point source microscope which is used as the ASM and a 5-axis milling machine was tested.

It should be noted that, in some areas of manufacturing, the requirements for stringent SI traceability of all measurands necessary for process control still cannot be met in all cases, such as in semiconductor manufacturing using projection lithography. In these cases, however, length and coordinate references are often taken from reference patterns of prior process steps or from existing mask artefacts (in-house "golden" artefacts), which have shown to be sufficiently stable, e.g. as in the case of quartz mask substrates [103].

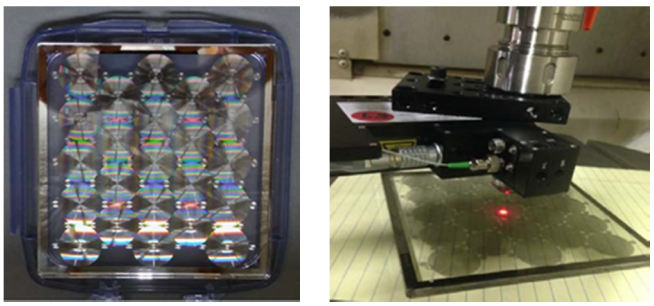

Figure. 8. Left: virtual 3D ball array CGH. Right: CGH on table and point source microscope mounted in the spindle of a 5-axis milling machine [227].

3. Dimensional artefacts for different measurement tasks

This section examines the state-of-the-art artefacts that are available for the main different categories of dimensional measurements. The artefacts are grouped according to the length service classification scheme, generally referred to as the "DimVIM" [27], which provides a harmonised terminology approved by the CCL. Consequently, the section is organised into four sub-sections, each one describing a group of artefacts, as follows: linear dimensions (Sect. 3.1), form and surface texture (Sect. 3.2), complex geometry (Sect. 3.3), and angle (Sect. 3.4).

3.1. Linear dimensions

This section covers linear dimension artefacts. The introductory part of this section defines general concepts, some of which are also useful for artefacts described in the following sections. Afterwards, the section continues with the description of the different types of linear dimension artefacts (gauge blocks, step gauges, etc.).

Measurement standards of linear dimensions are defined as those providing a reference (calibrated) length, or a sequence of them. A length is defined as the distance between two reference points. In artefacts with a sequence of calibrated lengths, the reference points all lie on a common line and the reference values are their abscissae along an axis aligned to such line from a common origin.

Even if linear dimension artefacts are intended to be 1D, they are objects in space and, therefore, are actually 3D, since they occupy a volume in space. At least for alignment purposes, elements or points off the measurand line are necessary (e.g. on lateral faces of step gauges), which makes a pure 1D definition and measurement impossible. This definitional issue is resolved in a recent document from the CCL, which sets the limits on CMCs to be considered 1D. A requirement is set on the *auxiliary measurements* (i.e. those made for alignment purposes only) to "*contribute small uncertainty, that is, reducing their uncertainties to nought would reduce the combined calibration uncertainty no more than 10 %*" [14].

Linear dimension artefacts are often used with multiple orientations in space, e.g. to verify the performance of coordinate measuring machines (CMMs) [147]. In addition, they may be combined in a rigid set up to form a full 3D artefact, such as a tetrahedron (see an example in Figure 44). In principle, the coordinates of their vertices (3D measurands) can be derived from the lengths of their edges (1D measurands). This is possible for tetrahedrons (and for triangles in 2D) because of their very property of possessing an equal number of degrees of freedom (DOF) and of edges ($3V - 6 = 6$ for tetrahedrons and $2V - 3 = 3$ for triangles, where V is the number of vertices), thus enabling a unique derivation of the vertex coordinates from the edge lengths. For other configurations, the resulting 3D artefact would be either under- or over-constrained, and for the purpose of this paper, they are not considered linear dimension artefacts.

Three items are particularly important for realising well-defined measurands: reference points, alignment, and origin. The definitions of the measurands should be unambiguous and insensitive to (reasonable) deviations from nominal geometry at the level of the best attainable uncertainty of measurement. In the same way as well-established measurement standards have to realise unambiguous measurands, attention is required in designing novel artefacts for specific purposes, so that unambiguous measurands are always realised (see also Sect. 5).

Reference points – Points are theoretical entities not existing in practice. Their definition is a specification operator [155] made of operations such as intersections (e.g. of a plane with a straight line for end standards), derivation of features (e.g. the sphere centres for ball bars), and projections (e.g. of a relevant feature onto a plane for artefacts involving imaging). The accurate definition and implementation of the reference points is key, particularly for high-accuracy and complex geometry artefacts. The definition of reference points is the equivalent for dimensional artefacts to the resolution for indicating instruments.

Alignment – A straight line possesses four DOF in space, of which two are translational in a plane, and two rotational about the two axes normal to the line. An imperfect definition or implementation of either type of DOF for the measurand line results in specific errors. The effects of rotational errors are called cosine errors [162] due to their proportionality to $1 - \cos\beta \approx \beta^2/2$ (valid for small β, where β is the misalignment angle). The features used for alignment (datums) should have negligible form error and high-quality surfaces, and be of sufficient size. In typical cases, the alignment is dominated by the face size or by the artefact length depending on whether the measurand line is defined orthogonal to the face or parallel to a longitudinal feature, respectively. The effects of translational errors arise from lack of invariance to lateral translations. For example, imperfect straightness or parallelism of the lines of a scale brings sensitivity to the later localisation of the measurand line. The accuracy requirement depends on the geometrical quality of the artefact. Fiducial marks (also called fiducials) may be provided for alignment.

Origin – The measurands of multiple length artefacts (i.e. having multiple reference points at linear positions p_i) are the reference point abscissae (x_i) relative to a common origin (p_0), $x_i = p_i - p_0$. The origin can be regarded in terms of DOF. The independent distances along an axis of a set of N points are $N - 1$ (e.g. one for two points); the common origin effectively subtracts the missing DOF. The origin p_0 brings correlation among the abscissae due to the common zero error. The distance of any reference point i to the origin is $d_{i0} = x_i = p_i - p_0$, while the distance to any other point j is $d_{ij} = x_i - x_j = (p_i - p_0) - (p_j - p_0) = p_i - p_j$. The origin does not affect point-to-point distances. Uncertainty-wise, this can be regarded as an effect of the (advantageous) correlation, which cancels the uncertainty component due to the origin. A typical choice for the origin is simply a reference point, usually the first in the series. This choice attributes an exceptional role to this point: its abscissa is null by definition with no uncertainty. This uncertainty though carries over to all other reference points. An optimal choice for the origin would be instead the reference points' centroid, i.e. the mean of all abscissae: the resulting uncertainty component due to the origin would be averaged and reduced by $\sqrt{N}$. The choice of the origin simply at one reference point is usual in calibrations; the choice of the centroid is advantageous when sets of repeats are either compared or averaged. Translating the origin to the centroid of each repeat prior to comparisons or averaging, and then possibly translating it back to a reference point, minimises the resulting uncertainty and is then recommended.

Gauge blocks

Gauge blocks (Fig. 9-a) are end standards, and are the most established and historical measurement standards of length. They were invented in 1896 and patented in 1901 [164] by the Swedish machinist Carl E. Johannson (Fig. 9-b). While selling gauges to different countries, he realised the importance of *one* standard reference temperature value. For manufacturing, he chose the round average of those adopted world-wide, 20 °C [79]. This became an important choice, as it was later endorsed internationally by the CIPM in 1931 and by ISO in 1954, and is today recognised as the global standard reference temperature for dimensional specification and metrology, according to the ISO 1 [140], [234].

(a) (b)

Figure 9. (a) A set of gauge blocks. (b) Johansson receiving the degree of Honorary Doctor of Science at Gustavus Adolphus College, USA, in 1932.

Gauge blocks are provided in sets of harmonised lengths, whose combination results in an evenly distributed sequence of lengths. Typical materials are steel, ceramics (particularly zirconia) and tungsten carbide (see Table 1). Steel is by far the most used, since it is cheap and makes the differential thermal expansion with most manufactured parts often negligible. Ceramics or tungsten carbide may be a better option for intensive use or in abrasive or corrosive environments. The secular stability of gauge block materials has been investigated by many authors (e.g. [195], [242]).

Gauge blocks are fully standardised by the ISO 3650 [144], which establishes definitions and tolerances in grades. The central length is defined as the distance of the central point of a measuring face to the plane of a platen wrung to the other face. This definition is suitable for interferometric calibrations but not for contact applications. In the case of contact measurements, one of the two reference points is the intersection of the perpendicular line with the measuring face, rather than with the wrung plane. When this face is not perfectly flat, and specifically when its central point is worn due to repeated contacts, the interferometric measurand and the length measured by contact may differ. Today's best calibrations offered by NMIs (see Table 2) are all by interferometry, which provides direct traceability to the metre. The underpinning theory of gauge blocks is described elsewhere (e.g. [78], [194]) and many interferometric set ups are reported (e.g. [32], [40], [43], [134], [136], [200], [291]). Some authors have introduced measuring principles other than phase-measuring interferometry, including optical frequency combs [161] and remote calibration by means of optical fibres [205].

The wringing of gauges is time consuming and may result in additional uncertainty. Several wringing-free double-ended set ups exploiting the two measuring faces directly as interferometric mirrors have been reported (e.g. [1], [180], [182], [277]). However, the wringing thickness is not included in these measurements while it is in the ISO 3650 definition, and a correction is needed. ISO 3650 sets a separation between short and long gauge blocks (sometime referred to as length bars). The central length (L) is defined with the gauge resting upright on a wrung face for the former, horizontal on two symmetrical points $L/\sqrt{3}$ apart for the latter (the Airy points, which preserve the parallelism of the faces in spite of the gravity, see Sect. 5). Examples of interferometric calibration set-ups are found in [17], [35], and [125]. The uncertainty in the calibration of long gauge blocks is mostly dominated by thermal expansion and air refractivity. A comprehensive survey of the uncertainty components in gauge block calibration is found for example in [74], while an authoritative guidance for calibration with mechanical comparison is given in [87].

Table 1.
Comparison of material properties for gauge blocks.

Property	Steel	Ceramic (ZrO_2)	Tungsten carbide
Thermal expansion /(10^{-6} K^{-1})	11.5	9	4.5
Thermal conductivity [(a)]	1	2.2	1.5
Resistance to corrosion	•	••••	••
Resistance to wear	•/••	•••	••••
Resistance to scratches	•/••	••••	•••
Resistance to shocks	••/•••	•	••••
Wringability	••/•••	••••	•••

•••• excellent; ••• good; •• fair; • poor.
[(a)] Soak-out time: ratio to steel.

Step gauges

Step gauges provide a sequence of parallel flat faces. The reference points are the intersections of the faces with a nominally-orthogonal straight line. Most step gauges are assemblies of a steel supporting beam and a sequence of steel or ceramic reference elements, such as gauge blocks or reference cylinders (Fig. 10). A monolithic ceramic prototype was manufactured for a recent key comparison [90].

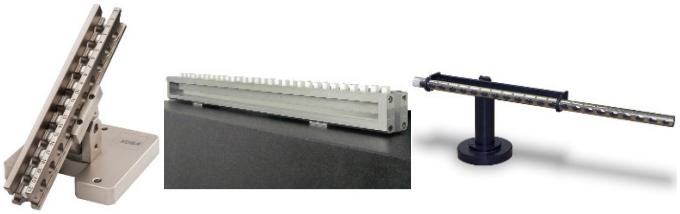

(a) (b) (c)

Figure 10. Various designs of step gauges. (a) The reference elements are on the neutral axis; good accessibility is achieved by a heavy asymmetrical cross section (source: Kolb & Baumann). (b) The measurand line is off the neutral axis and the reference elements must be decoupled from the supporting beam (source: Mitutoyo). (c) The step gauge shows good symmetry and is lightweight, but probing would be obstructed and windowing is required (source: MDM Metrosoft). The measurand lines are (a) the translated intersection of two lateral sides; (b) the translated normal to the front surface, (c) the axis of the cylindrical beam.

Step gauges are mainly used in performance verification of CMMs according to ISO 10360-2. They are also used for setting height meters, usually in the vertical position. The measuring faces of step gauges point either in the positive or in the negative direction along the measurement line, and can realise both unidirectional and bidirectional measurands (see Fig. 5). The probing of the reference points depends on the stylus tip diameter; very often, the resulting calibration errors show an oscillation between positive and negative faces (e.g. [167]). The mutual shadowing of the aligned faces requires contact probing with later disengagement to get access. To comply with the Abbe principle (reference and sensing points aligned to the measurement direction [191]), different set ups have been proposed. Two wide flat mirrors are often attached symmetrically to the probing system; their mean is Abbe compliant and the interferometric counting is not broken while disengaging [42], [224], [274]. Miniature step gauges for testing non-contact CMSs, featuring high surface cooperativeness and dimensional stability, were introduced in [72] and further developed in [7], [45] and [290].

Ball bars

Ball bars are made of two spheres spaced by a bar (Fig. 11 left), or by an array of aligned spheres, also called multi-ball bars (Fig. 11 right). Their reference points are usually defined as the sphere centres, disregarding the diameters. The reference points of ball bars with two spheres may also be defined as the opposite poles, i.e. the outmost intersections with the straight line through the centres. Depending on the two different definitions, the two resulting measurands differ by the mean diameter of the two balls. According to ISO 10360-2, the former definition supports unidirectional and the latter bidirectional measurements, which are insensitive or sensitive, respectively, to probing errors.

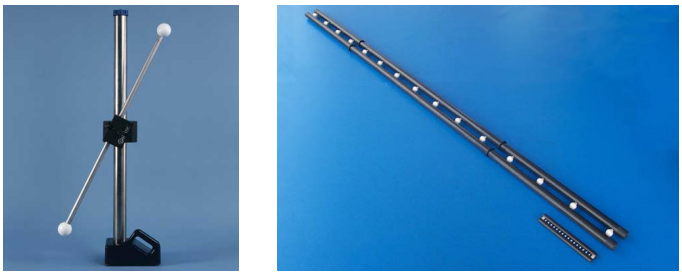

Figure 11. Ball bars of different designs and sizes. Left: two-sphere ball bar (source: Micro Surface Engineering). Right: multi-ball bars of different lengths – 1.4 m and 120 mm (source: Trapet Precision Engineering).

The main use of ball bars is in performance verification of CMMs, according to ISO 10360-2. They were introduced in the current version of the ISO standard to cover their popular use, particularly in the USA [10], [233]. Some are telescopic with their balls kinematically constrained to the table and to the ram for evaluating and/or compensating the geometry errors of CMMs and machine tools [262]. These are in fact indicating instruments in combination with an artefact. Ball bars cover a wide range of sizes (see Figure 11).

Diameter standards

Diameter standards, in the form of cylinders, can be considered linear dimension artefacts when the measurand is defined as a point-to-point diameter. The reference points lay on an intersecting plane orthogonal to the cylinder axis, at a predefined position, and are aligned to fiducials [88]. Very often, instead, the intersecting plane is taken parallel to a reference face (cylinder base), particularly for rings. Diameter standards can also be calibrated for form (roundness, straightness, cylindricity); see Sect. 3.2. The combination of diameter and form calibrations results in full 2D (or 3D) measurement standards. Their use as primary measurement standards is mainly for traceability in calibrations by comparison with secondary measurement standards. As for step gauges, a disengagement is needed. Alternative solutions have been proposed complying with the Abbe principle [171], [231].

Line scales

Line scales are arrays of regularly spaced marks on a flat substrate (see Fig. 4). The reference points are defined as the intersections of the scale lines with the measurand straight line. The measurand straight line is defined on the upper surface by fiducials. The reference points are defined based on features (cross-section profiles) either below the surface (engraved) or above (printed, typically by lithography); in either case, these are 2D features while reference points are sought. An association operation [154] is required to reduce the 2D features to points. The reduction of the horizontal dimension is critical as it affects the measurands directly. Possible options are by taking the midpoint of the line edges, or the mean value of the line profile. The former is not affected by the interior of the profile, but the edges are never perfectly sharp; the convolution occurring in line sensing results in imperfect geometry when smoothing the detected profile. The latter relies on sensing the line rather than on the geometrical feature itself. The reduction of the vertical dimension is achieved by projection onto the measurand straight line. This is less critical than the horizontal, even though possibly affected by parallax (the common origin cancels the error component common to all lines). The definition of the measurand is much improved by coupling a reading head permanently, as done for linear encoders. This makes these artefacts indicating instruments. Linear encoders are mentioned here among the linear dimension artefacts, although they are “active” instruments (see Sect. 1), for their similarity to line scales and because they are so categorised in the DimVIM [27]. The reading head of linear encoders is usually equipped with a short line scale with the same design as the main scale. When sliding over one another, a periodic signal is obtained (optically, magnetically, interferometrically, by diffraction, or by other means) with the same period as the scale pitch. Linear encoders not only can compete in accuracy with direct interferometry (see Sect. 2, [178] and [105]), but are also practical, robust, and fit for applications in harsh environments. Today’s CNC machine tool and CMM axes are typically equipped with linear encoders. A new generation of encoders (see e.g. [12]) addresses one of the main drawbacks in comparison to laser interferometers, i.e. the inability to align the measurement axis of the encoder with the point of interest. These new designs address this drawback by providing limited displacement measurements over a small range in a direction orthogonal to the primary measurement direction, which allows for the measurement and compensation of Abbe errors and enables the Abbe compliant measurement of straightness (see Sect. 3.2). On the other hand, the passivity of line scales enables their use in performance verification of active (indicating) instruments, such as optical CMMs [148]. High-accuracy instruments for the calibration of line scales and linear encoders are described elsewhere (e.g. [36], [285]). High-accuracy line scales made of low-expansion materials are used for comparing world-wide measurement capabilities [37].

Linewidth standards

The measurand of a linewidth standard is the width of a single line marked on a flat substrate. The reference points are the edges of the line in a predefined direction. Linewidth standards are similar to line scales, but with a different aim: width (which is a feature of size) is measured in linewidth standards, while position along the axis is measured in line scales. A reference line scale is not sufficient for measuring features of size, such as the diameter of a disk or bore, and must be complemented with a linewidth standard. In ISO 10360-7 [148], a single line scale can be used for performance verification of optical CMMs provided that its lines are measured bidirectionally, i.e. by taking the reference points on the opposite edges of any line pair. The linewidth measurand is very sensitive to the sensing mechanism; therefore, a same linewidth standard may result in different calibrated values depending on the sensing technology used [267] (see also Sect. 2 and Figure 5). A photomask measurement standard based on a 152 mm square quartz mask substrate carrying chromium line structures from 5 µm down to nominally 40 nm CD was designed for linewidth calibration and successfully used in a round robin exercise on measurement systems used in semiconductor and photomask industry [103]. The mask design has been applied to manufacture several CD measurement standards using up-to-date manufacturing technology of mask shops in Germany.

1D gratings

As with line scales, gratings are arrays of regularly spaced marks on a flat substrate, but the pitch is much smaller and comparable to the wavelengths of visible light. When illuminated by coherent

light, they give rise to diffraction. The measurand is the pitch p of the grating, either mean or local. The mean pitch sets the diffraction angles θ_m according to the equation $p \cdot \sin\theta_m = m\lambda$ (m is the diffraction order and λ is the light wavelength). The local pitch is used for correcting microscopy instruments, such as AFMs. Usually calibrations take the mean pitch as the measurand (see e.g. [73], [108], [255]), while the local pitch is most likely used in applications. The diffraction profile depends on the full grating profile, i.e. the off-peak non-null intensities bring information on the deviations from regular periodic geometry [213], which in principle could be derived (but in practice is seldom done in actual calibrations). The regularity of the grating is important for traceability when the calibrated mean pitch value is used for local pitches.

Ball/hole plates and 2D gratings

Although ball/hole plates and 2D gratings are not 1D artefacts, they are covered here for their similarity with ball bars and 1D gratings, of which they can be considered as 2D extensions. In general, the measurands are the coordinates of the reference elements. These are 2D vectors whose deviations from the nominal depend on, but cannot be confined to, the linear errors of the two axes. Specific 2D issues arise, most prominently the squareness and the definition of a local system of coordinates. This latter is usually based on three reference points that define a coordinate plane, two of the three a coordinate axis, and one of the two the origin. In the case of 2D gratings, the reference points (marks) are very many (with a short pitch), and a full calibration of their individual coordinates would be impossible and useless in practice. Reduced measurands, such as the average pitches and the squareness, are measured instead.

Ball and hole plates are assemblies of supporting plates with a 2D array of reference elements, spheres or cylindrical holes. The reference points are the centres of the balls or of the circular cross sections of the holes at a predefined depth, respectively. The supporting plates are usually made of steel, or of low-thermal expansion materials. Ball and hole plates are mainly used for 3D verification of CMMs and for derivation of their geometry errors [15]. Figure 12 shows a dedicated hole plate that was designed and manufactured for multi-sensor opto-mechanical CMMs [121]. Ball/hole plates are routinely calibrated according to the swing-round procedure [15], which eliminates most geometry errors of the calibrating CMM (except the high-order odd parts of the scale errors). The design of ball/hole plates allows access from either side intentionally for this purpose (see Figure 42-c, where a typical cross section of a ball plate is shown). Other 2D artefacts similar to hole plates are available, such as mask substrates carrying chromium structures (e.g. circles), analogously to the chromium line structures used for some linewidth standards (see above). The particular challenges for calibration of bidirectional measurands such as diameters of holes or circles on substrates were discussed in Sect 2.

2D gratings are 2D arrays of regularly spaced marks on a flat substrate. The measurands are the average pitches and the orthogonality of the axes. These artefacts are used mainly for performance verification and calibration of microscopes and 2D stages [101]. They can also be used as the basis for 2D encoders [172], for 3D interferometric sensors [106] and for full 6 DOF encoders [197]. 2D gratings are usually calibrated by either diffractometry or scanning probe microscopy (SPM) (typically AFM) [109], [193]. Suitable vision algorithms help in aligning the artefacts [201] and in suppressing the noise [54]. Detailed analyses of the diffracted wavefront can be used for deriving flatness information [55], [107]. The CMCs registered in the KCDB (Table 2) for these artefacts report uncertainties as low as 2 pm (for 23 nm pitches, shortest in the range). An intercomparison demonstrated capabilities at the 10 pm level [100].

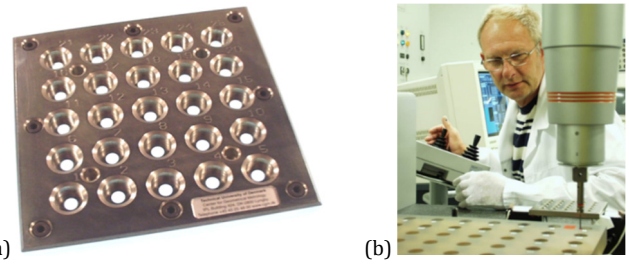

(a) (b)

Figure 12. Opto-mechanical hole plate allowing to link optical and tactile measurements into the same reference system on a multisensor CMM [71]. (a) Hole plate with 25 × ø5.5 mm holes. (b) Transfer of traceability from a Zerodur hole plate.

Table 2.
Best CMCs (calibration and measurement capabilities) for linear dimension artefacts. U is the expanded uncertainty (k = 2). Q[a, b] is a short form for $\sqrt{a^2 + b^2}$. L is the nominal length of the measurand (source: KCDB [29]).

Artefact	NMI	Range (mm)	U
Gauge blocks	SMD (BE)	0.1 – 100	Q[18 nm, 0.15 × 10^{-6}L]
	NIST(US)		
	PTB (DE)	100 – 1 000	Q[22 nm, 66 × 10^{-9}L]
Step gauges	NPL (GB)	10 – 1 540	Q[0.1 µm, 0.23 × 10^{-6}L]
Ball bars	NIST(US)	300 – 1 500	Q[0.25 µm, 0.5 × 10^{-6}L]
Rings	PTB (DE)	10 – 170	Q[14 nm, 0.1 × 10^{-6}L]
Line scales	MIKES (FI)	0.01 – 1 165	Q[6.2 nm, 82 × 10^{-9}L]
Linewidth st.	PTB (DE)	0.002 – 1	15 nm
Ball/hole plates [a]	METAS (CH)	1 – 80	Q[0.03 µm, 0.2 × 10^{-6}L]
	NMIJ (JP)	0 – 560	Q[0.24 µm, 0.56 × 10^{-6}L]
	PTB (DE)	0 – 960	Q[0.4 µm, 0.5 × 10^{-6}L]
		Range (µm)	
1D gratings [a]	NMIJ (JP)	0.023 - 8	Q[34 pm, 19.8 × 10^{-6}L]
	NIST (US)	0.1 - 10	Q[3 pm, 2 × 10^{-6}L]
	NMC (SG)	0.05 - 50	Q[60 pm, 1.2 × 10^{-6}L]
2D gratings [a]	PTB (DE)	0.007 – 0.223	Q[2 pm, 0.03 × 10^{-3}L]
	PTB (DE)	0.14 – 4	20 pm
	METAS (CH)	0.3 – 10	Q[6 pm, 9 × 10^{-6}L]
	MIKES (FI)	0.287 – 10	Q[52 pm, 11.6 × 10^{-6}L]
	METAS (CH)	0.2 – 20	0.05 × 10^{-3}L
	NPL (GB)	0.29 – 50	Q[25 pm, 0.19 × 10^{-3}L]

[a] These CMCs are best in different ranges.

3.2. Form and surface texture

Form and surface texture definitions and measurements are discussed in detail elsewhere (for example, surface form in [93] and surface texture in [287] and [186]). The main types of artefacts available are described below.

Flatness measurement artefacts

The reference geometry for flatness is the plane, hence flatness is the degree to which the measured surface deviates from a plane [124]. ISO 12781-1 [151] provides more details on flatness specifications. One method to measure flatness is by probing the surface with a CMS. However, measurement by CMS can be a time-consuming task as surface points are acquired sequentially in most cases. A widely accepted method for flatness measurement is using optical interferometry, where the surface to be measured is compared to a calibrated reference flat, but deflectometry can also be employed [110]. Self-calibration and reversal approaches can be used to enhance the accuracy of flatness measurement so that nanometre-level uncertainties are readily achievable [91] [93] [238]. The reference artefacts for flatness measurement are often optical flats, although for lower accuracy applications, surface plates and tables can be employed, and most NMIs have flatness measurement services. Sometimes the size of the flat area to be characterised (e.g. granite bases of CMMs and machine tool tables) means that other flatness measurement methods must be employed, such as electronic levels arranged in a surface grid (see

e.g. ISO 230-1 [141]). Optical flats are commercially available in a range of materials and sizes, and can be calibrated simply by using a He-Ne laser and self-calibration techniques, without the need for external traceability to an NMI [190]. Particularly high-specification flats were produced for the LIGO gravitational wave detector, which had peak-to-valley flatness values of 0.37 nm (with reference to a least-squares plane) over a 150 mm aperture [232]. Liquid surfaces are also used as flat references, although there are obvious practical difficulties in maintenance and calibration [235].

Optical flats are used for the calibration of the residual flatness metrological characteristic for surface texture instruments, but care must be taken that the appropriate spatial frequency distribution is employed – typical flatness calibration services use full-field interferometric systems where the lateral sampling spacing is likely to be too large for surface texture applications [115] (a similar argument based on the finite probe geometry can be employed in the case of a CMS measurement).

Straightness measurement artefacts

The reference geometry for straightness is a line, defined as the shortest path between two points in space. ISO 12780-1 [150] provides more details on straightness specifications. The most common measurement methods for straightness are autocollimators, laser interferometers or electronic levels, although CMS can be employed for lower accuracy applications. Artefacts for straightness references include flats, dedicated mechanical beams (straightedges, used for lengths up to approximately 5 m – see Sect. 5 for details on the effects of gravity and fixturing especially on long artefacts) and taut wire artefacts (mostly used for lengths over several metres – where the uncertainty of straightness measurement in the vertical direction increases with length, due to sag of the taut wire) [141]. See Figure 13 for an example. A relatively new type of artefact is the holographic axicon [226], which can be used to measure straightness in two directions simultaneously, establishing a virtual optical line of reference perpendicular to the plane of the axicon. This virtual line can be probed with an autostigmatic microscope (see Sect. 2) with sub-micrometre resolution and is less susceptible to air turbulence than a single laser beam.

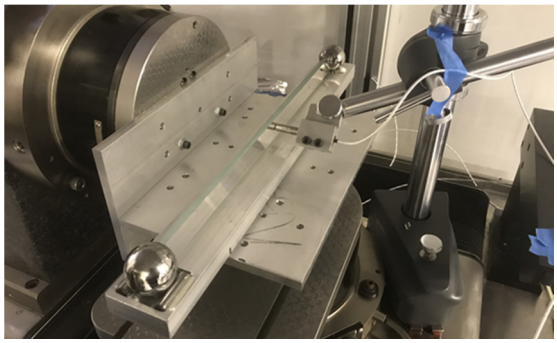

Figure 13. Example of a straightedge measurement on a machine tool using a reference beam and a capacitance gauge [223].

Roundness and cylindricity measurement artefacts

The various parameters for roundness and cylindricity characterisation are well established and their definition and standard measurement methods will not be repeated here (see [143] and [93]). The highest accuracy measurements of roundness and cylindricity are carried out by dedicated roundness measuring machines, but CMS can also be used in lower accuracy applications. The most common reference artefacts for roundness are precision spheres or hemispheres (see Figure 14-left), usually calibrated by reference contact instruments. Self-calibration and reversal approaches, often employing multiple probes, can be used to enhance the accuracy of roundness and cylindricity measurement so that tens of nanometre-level uncertainties are achievable [91] [56] [93] [123]. Precision cylinders are also used for roundness and cylindricity characterisation. Figure 14-right shows a typical cylinder roundness artefact. A roundness artefact has been developed with different regions [122], which facilitates calibration of the amplification factor of the probe [166], the dynamic properties of the probe and investigation of various filtering methods employed. On a larger scale, a ring segment artefact has been developed for traceability of large diameter bearing components (up to 1 m in diameter), which composes two nominally coaxial features: a cylinder and a torus [16].

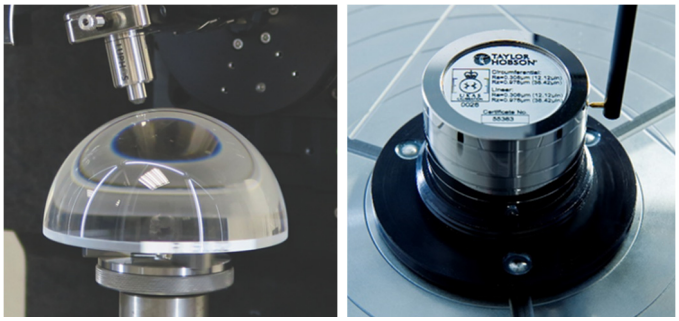

Figure 14. Examples of roundness artefacts (source: Taylor Hobson). Left: precision hemisphere being measured with an optical instrument. Right: a typical cylindrical roundness artefact being measured with a stylus instrument.

Spherical and aspherical form measurement artefacts

The most obvious choice for an artefact for characterising measuring instruments for spherical form is a precision sphere, or more often, a hemisphere (see Figure 14-left for an example). Such artefacts are made from a variety of materials, but the highest precision are made from optical glasses. Spherical artefacts can also be used for spindle error assessment [203] and are commonly used in conjunction with other artefacts as datums, reference features and alignment aids (see e.g., Figures 21, 24 and 26). For surface texture measuring instruments, a precision hemisphere on a plane artefact (known as a Type E1 material measure for profile [145] and a Type APS material measure for areal [157]) is used for assessing multiple parameters, such as vertical and horizontal scales, the squareness of the lateral axes, the response curve of the probing system, the stylus geometry and stylus tip geometry [190]. Precision spherical artefacts are most often calibrated using primary roundness and/or profile measuring instruments, typically to form uncertainties of a few tens of nanometres. The highest precision spherical metrology to date has been for the silicon sphere produced for the redefinition of the kilogram using the Avogadro method [18], which produced a 93.6 mm diameter sphere to form uncertainties of less than 20 nm, measured with a spherical cavity Fizeau interferometer and resulting standard uncertainty for the mean diameter of 0.22 nm [219] [220].

Aspheric optics play an increasingly important role in a wide variety of optical applications. The requirements placed on the quality of advanced aspheres are high and their production accuracy is limited by the available measurement techniques [92]. Most commercial aspheric measuring instruments are supplied with spherical reference artefacts, but there has been some activity, mainly in the NMIs, to develop aspheric artefacts. In 2018, PTB led an interlaboratory comparison of asphere measurement, in which a weak asphere, strong asphere and a sample with two radii in orthogonal directions were measured using a number of high-accuracy contact and optical techniques [256]. In this comparison, there was no traceable reference instrument, so virtual references were used and the results only show variation between instruments. RMS deviations were found to be of the order of tens of nanometres, up to 90 nm in the case of the strong asphere. There have been several advances in optical technologies

for asphere measurement (see e.g., [13], [129]) and contact CMSs can be employed (e.g., see [26], [288]). Traceability for these instruments is now in place, thanks to developments in the EMPIR project FreeFORM (see [9] for a summary of the project outputs). There is much cross-over from asphere metrology developments and precision freeform metrology developments, which are discussed in Sect. 3.3.

Surface texture artefacts

In the case of surface texture instruments, there is a comprehensive framework for calibration and verification under development in ISO technical committee 213 working group 16 (ISO/TC 213/WG 16). A number of defined metrological characteristics are determined using default procedures and artefacts which were described in detail in a previous CIRP keynote [190], so this detail will not be repeated here. Since that keynote, ISO 25178-600 [158] has been published, which lists and defines the metrological characteristics. ISO 25178-700 will describe how to determine the metrological characteristics and should be published soon. CIRP STC-S is currently conducting a comparison of the ability to measure one of the metrological characteristics, instrument noise. There have been some developments in the manufacture and calibration of artefacts used to determine the linearity of the instrument scales, including a grid artefact for focus variation microscopy [2], which has the added complication of requiring a rough surface, and a diamond turned surface with pseudo-random texture, where the analysis uses the material ratio curve to determine the axial scale linearity [83].

The National Physical Laboratory (NPL) [222] and University of Kaiserslautern (UOK) [84] have independently developed multi-feature artefacts that allow the determination of the ISO 25178-600 metrological characteristics, with the exception of topography fidelity (see below). NPL offer the artefact shown in Figure 15 on a silicon substrate along with separate performance verification artefacts on nickel electroformed substrates [189]. The UOK artefact is manufactured by stereolithography, with a metal coating, and is currently subject to an intercomparison managed through ISO/TC 213/WG 16.

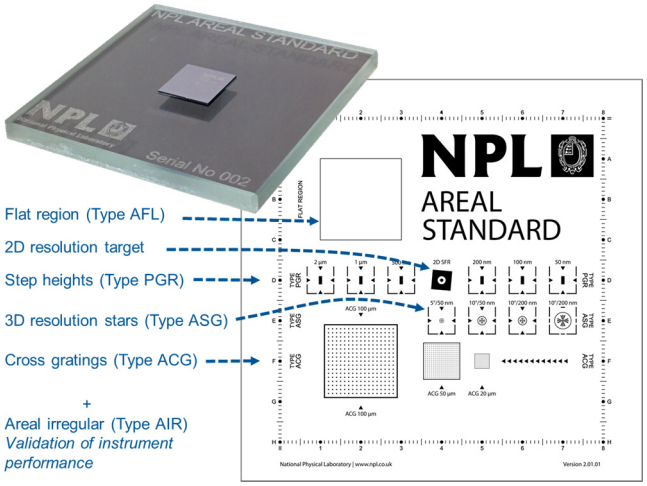

Figure 15. The NPL Areal Standard (source: NPL). Top-left: picture. Bottom: scheme with explanation of the various features.

A metrological characteristic "topography fidelity" has been introduced into the ISO framework as a kind of miscellaneous category for all contributions to the uncertainty budget, including surface slope-dependent errors that are not captured by the more well-known calibrations. In ISO 25178-600 [158], topography fidelity is defined as the *"closeness of agreement between a measured surface profile or measured topography and one whose uncertainties are insignificant by comparison"*. A common theme is to use an artefact having a shape that is identical to the measurand, and that has been calibrated independently and/or manufactured in such a way that the real geometry is known. For example, one part could be manufactured and used as a reference for all subsequently manufactured parts of that shape. Measuring this artefact using the instrument to be evaluated may give quantitative information about the deviations that can be used in an uncertainty budget. Artefacts are under development for topography fidelity that include a multitude of established difficult-to-measure features, such as steep steps and grooves of various spacings and depths. Example artefacts under development include the chirp standard [264] that is comprised of square-waves of varying lengths and depths, and a circular chirped specimen with several degrees of randomness in lateral size [65], see Figure 16, which shows measurement results with the artefact – the clear over-/under-shoot features are what the artefact is designed to illustrate.

There has also been some progress in the development of artefacts for the determination of transfer function, which is one of the elements encompassed by the definition of topography fidelity, but which can also be used to establish topographic resolution. Care must be taken to distinguish the instrument transfer function (ITF) and the optical transfer function (OTF) (see [75] for a comparison of the two functions). Methods and artefacts to determine ITF are common in the optics industry and the limitations are well understood. Use of the OTF addresses some of these assumptions, but its adoption is less well advanced. Recent suggested artefacts for OTF (with associated models) include a precision micro-scale sphere [272], the chirp artefact discussed above [264], a pseudo-random artefact [170] and a star-pattern produced using lipid biolayers [25]. It should be noted that the PTB circular chirped artefact [65] has been suggested as an artefact that can be used to determine the ITF of an optical instrument, but, with its current design, it will produce results that are outside the linear assumptions inherent in the definition of the ITF. However, at the time of writing, there is no consensus on how transfer function and/or topography fidelity should be determined or even if it is possible to do this with single artefacts [188]. The current situation in ISO 25178-700 is that topography fidelity and transfer function will not be part of the normative sections.

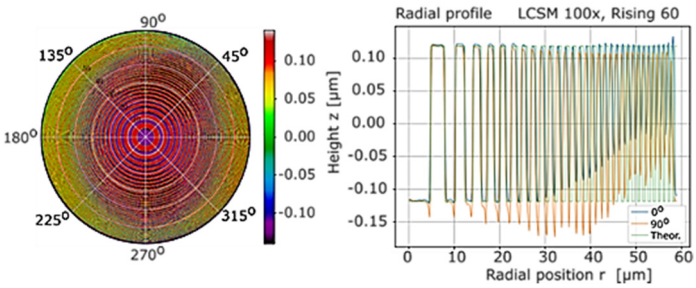

Figure 16. Topography fidelity artefact designed by PTB [65]. Topography data map of the circular chirp pattern (radius of 60 µm) measured by a commercial laser scanning confocal microscope with a 100× objective (left) and its profiles along the orientation of 0° and 90° (right).

With the publication of ISO 25178-600, the development of ISO 25178-700 and the availability of the multi-feature artefacts from NPL and UOK, the calibration of surface texture measuring instruments has advanced significantly. With many of the surfaces found in advanced manufacturing, the current framework is sufficient and can be used to evaluate measurement uncertainty, but there are still issues to address. Topography fidelity is a catch-all term that describes those aspects about a surface texture measurement that defy the simple linear models of the various instruments [188]. In these regimes, which are typical of complex surfaces, such as those found in AM, rigorous models are needed to allow a prediction of the response of the instrument to the

topography. Whilst there is some activity in this direction (see [276]), there is still much work to do before suitable calibration artefacts can be designed, manufactured and tested. There is also increasing interest in using X-ray computed tomography (CT) to measure surface texture [187], especially for highly complex surfaces, some even with undercut features. Artefacts for this regime of surfaces, essentially made using the manufacturing method under examination, calibrated using specific procedures and then measured with CT are in the stage of development [297].

3.3. Complex geometry

Complex geometrical features are defined in the ISO 17450-1 [154] as geometrical features that have no invariance degree. Measurements of complex geometries and freeform shaped parts were reviewed in a previous CIRP keynote [253]. Many different types of CMSs, ranging from tactile CMMs to non-contact CMSs, are commonly used in manufacturing metrology for measuring complex geometries [135]. Since CMSs are flexible measuring systems, capable of measuring a multitude of features and products, they are not calibrated for all the large number of measurement tasks that they allow, but they need task-specific calibration [289]. For the same reason, a large number of different artefacts have been developed to establish traceability in many different measurement applications. Artefacts used in coordinate metrology range from objects based on simple geometrical features to freeform shaped parts.

Artefacts based on simple geometrical features

Complex artefacts based on simple geometrical features typically combine several regular geometries, such as planes, cylinders and spheres. Besides linear dimension artefacts, already described in Sect. 3.1, several 2D and 3D artefacts have been developed for CMS verification and calibration [248]. Reviews of existing CMS artefacts are reported elsewhere (see [3], [59] and [245]). These artefacts can be used in single or multiple positions within the CMS measuring volume. Often, such artefacts include spherical features that can be accurately measured by CMS and used for alignment. Examples of such artefacts are shown in Figures 17 and 18. Figure 19 shows a "pseudo-3D artefact" [114] consisting of a 2D ball plate that is mounted on top of spacers of different heights using kinematic couplings, which ensure repeatable positioning of the plate to create a 3D lattice once measured by optical CMSs, such as fringe projection. The concept of using spacers was inspired by previous work by Bringmann et al. [39], in which a kinematic artefact was presented and applied for testing and calibration of machine tools. Other examples of artefacts for testing and calibration of three- to five-axis machines are reviewed elsewhere (see [266], [212], [207]). The use of finished artefacts for machine tools verification is detailed in the ISO standards on test code for machine tools [141] [142], while artefacts generated directly by manufacturing equipment are specified elsewhere (e.g. [149] for cutting machine tools and [159] for AM machines).

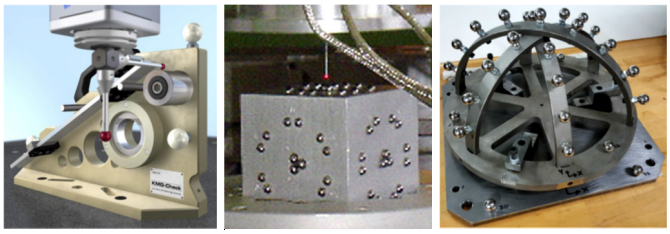

Figure 17. Examples of complex artefacts based on simple geometrical features, for coordinate metrology on CMMs or on machine tools. Left: "KGM-check" artefact (source: Carl Zeiss). Middle: Calibration of a parallel-kinematics probe using a "calibration cube" [292]. Right: "ball dome" artefact developed for five-axis machine tools used for coordinate metrology [207].

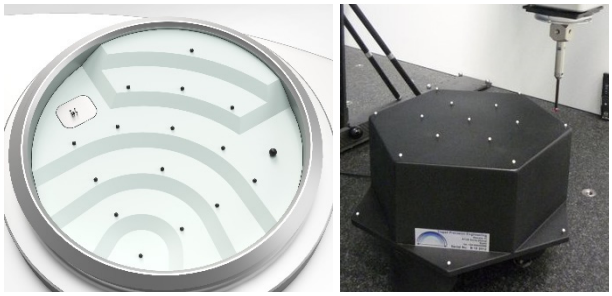

Figure 18. 3D artefacts made of glass or vitro-ceramics and calibrated ceramic spheres. Left: "amphitheatre-like" glass artefact with optically cooperative micro-spheres that have diameters down to 0.36 mm and are suitable for different tactile and optical micro CMSs [275]. Right: 3D artefact with 3 mm diameter spheres on low CTE vitro-ceramic material (source: Trapet Precision Engineering).

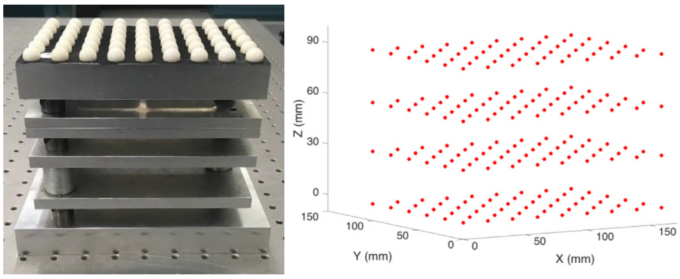

Figure 19. "Pseudo-3D artefact" [114] using a 2D ball plate and spacers of different heights (left) to create a 3D lattice once measured (right).

Freeform shaped artefacts

Artefacts based on freeform geometries use complex continuous surfaces in which the shape and the extension are defined by the designer to model freeform applications, which cannot be represented by regular geometries. For example, PTB proposed different freeform shaped artefacts, ranging from general-purpose sinusoidal shapes to application specific artefacts, for verification of optical CMSs [263]. Figure 20 shows the NPL freeform artefact, which features a 3D complex surface including both convex and concave forms [208].

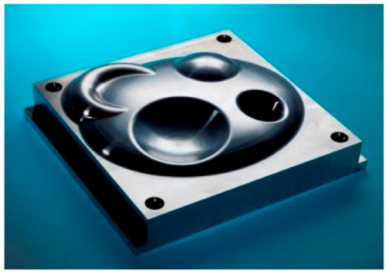

Figure 20. NPL freeform artefact [208]; the nominal dimensions of the model shown are 150 mm × 150 mm × 40 mm.

Figure 21 shows the "hyperbolic paraboloid" freeform artefact developed by the Czech Metrology Institute (CMI) [298]. This artefact was used by the CMI also for developing the so-called "calibrated CAD model" of the freeform object [198]. The idea of calibrated CAD was introduced by Savio et al. [254], in connection with the Modular Freeform Gauge reported below in this section. While in the work by Savio et al. the calibrated CAD was based on regular geometries used to substitute freeform shapes, in the work by the CMI the calibrated CAD model is based on iterative modification of the control points determining the theoretical shape of the freeform surface according to the data measured on the artefact [198]. The CMI demonstrated that the form errors evaluated in CAD-based measurements, where the calibrated CAD

model is used as reference, can be much smaller than form errors evaluated in CAD-based measurements of the same artefact with the nominal ("uncalibrated") CAD model used as reference [298].

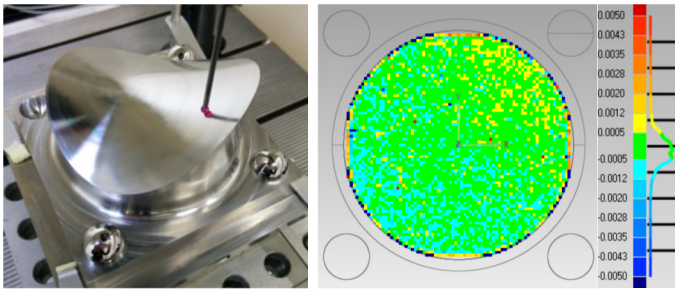

Figure 21. Hyperbolic paraboloid freeform artefact developed by CMI [198]. Left: artefact with maximum dimensions of 120 mm × 120 mm × 67 mm, consisting of step-squared base intended for clamping, an hyperbolic paraboloid surface trimmed by a cylinder of revolution with 40 mm radius, and three precise reference spheres with 8 mm radius that are glued into hemispherical holes on the artefact. Right: calibrated CAD model, with colour map of deviations between CAD and points measured using a tactile CMM.

Gear and thread artefacts

In order to ensure traceability of measurements of gears and threads, several product-like artefacts with complex geometries are available. For example, Figure 22 shows large involute gear measurement standards (with outside diameters of 1 m), which make possible the calibration of important gear measurands for profile and lead [3]. Other examples are reported in [119] and [181], where artefacts for micro gear measurements are presented, using spheres to resemble involute profiles and cylinders to resemble the involute tooth flanks. Further examples and details on gear artefacts are reported elsewhere (e.g. [116], [3], [280]). Calibrated thread artefacts have also been used for traceability transfer in newly developed screw thread measurement methods using contact and non-contact CMSs [47] [296].

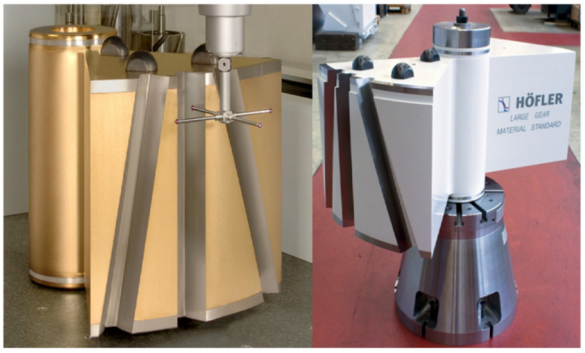

Figure 22. Involute gear measurement standards [3]. Left: PTB national reference standard. Right: industrial measurement standard.

Modular Freeform Gauge

Based on the substitution approach [152], the Modular Freeform Gauge (MFG) concept was proposed by Savio et al. [251][254], in which the freeform surface is substituted by the surfaces of simple prismatic objects, assembled in such a way that the complex shape of interest is simulated as closely as possible. The MFG concept has practical constraints with respect to feasible configurations and similarity requirements. The approach for traceability establishment is illustrated in Figure 23-left. An example of application to a turbine blade is shown in Figure 23-right; the geometry of the blade was simulated by an assembly of a cylinder and two flat surfaces, estimating a freeform measuring uncertainty of the order of 2 µm to 3 µm for contact scanning on a high-accuracy CMM [254]. Other examples of traceability transfer using the MFG concept are given elsewhere [102] [199]. Using a section of a wind turbine blade calibrated following the MFG approach, shown in Figure 24, an expanded uncertainty (k = 2) of 665 µm was documented for automated freeform optical scanner measurements of the leading edge geometry on a 55 m blade [199].

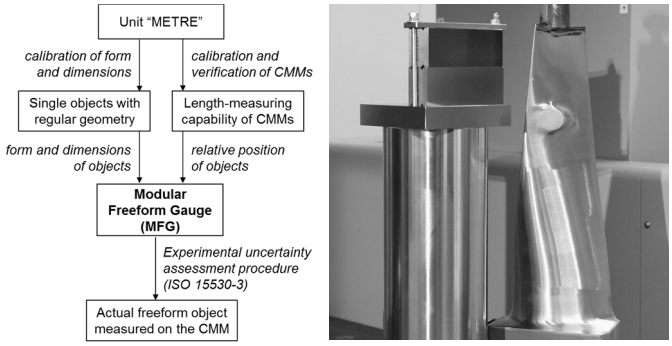

Figure 23. Traceability of CMM freeform measurements using Modular Freeform Gauges [254]. Left: flowchart illustrating the approach. Right: example of MFG configuration for the uncertainty assessment related to the measurement of a turbine blade.

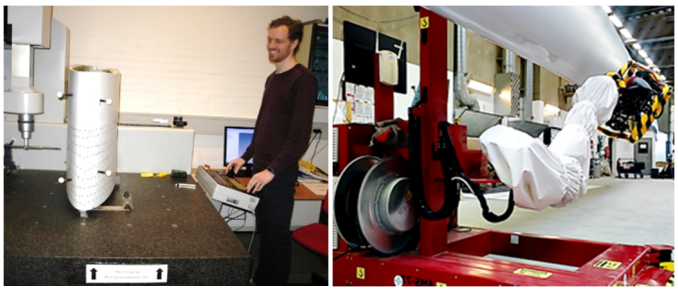

Figure 24. Establishment of the traceability of automated freeform optical scanner measurements on wind turbine blades in the production [199]. Left: calibration of freeform surface of a wind turbine blade section. Right: optical 3D scanner mounted on a 6 DOF robot with reference to a laser tracker during measurement of a 55 m wind turbine blade.

Artefacts for non-contact measuring systems

In parallel with the current trend to the increasing use of optical measuring systems and X-ray CT, several new artefacts have been developed by selecting materials and surface properties that facilitate the measurements of non-contact sensors (see Sect. 5).

As far as optical sensors are used, artefacts with optically cooperative surfaces are beneficial and for this reason several coatings and surface treatments, including Lambertian surfaces, have been developed and studied [81] [249] [275]. Further details on artefacts for optical sensors are discussed in Sect. 5, in the clauses on surface and optical properties. 2D artefacts for vision-based systems, such as hole plates and mask substrates carrying chromium structures, are discussed in Sect. 3.1.

Artefacts for X-ray CT are reviewed in [5] and [48]. Many artefacts used in tactile and optical coordinate metrology are not suitable for X-ray CT because they are made of highly absorbing materials (i.e. with high X-ray attenuation coefficient) such as steel. For this reason, several artefacts have been developed specifically for X-ray CT, using materials and X-ray penetration lengths adapted to the measurement parameters. Materials usually adopted for such artefacts include metals with low X-ray absorption, such as titanium and aluminium, as well as low absorbing ceramics and synthetic ruby. When connections between single objects are needed to form an artefact, they are often realised with carbon-fibre reinforced polymer as it is relatively X-ray transparent, yet it has good geometrical stability and low CTE [76]. Figure 25 shows two examples of artefacts made

from carbon fibre tubular structures on which a number of reference spheres are positioned at specific locations. The artefact in Figure 25-left was developed at the University of Padova for the geometrical calibration of CT systems [76]. The artefact in Figure 25-right was developed at the Technical University of Denmark (DTU) and is placed and scanned together with the workpiece inside the CT system, allowing a considerable reduction of time by compressing the full process of calibration, scanning, measurement, and re-calibration, into a single process [271].

Since different materials can strongly influence the results of CT measurements, multi-material artefacts have been developed [240] [160]. Polymeric materials have been proposed for X-ray CT artefacts because of their low X-ray attenuation coefficient and for use with same CT measurement parameters as with actual polymeric workpieces (see e.g. [45] and [206]). Experimental studies have investigated their use and limitations in terms of long-term dimensional stability, thermal expansion and influence on measurement uncertainties (see [206] and Sect. 5). Typical calibration uncertainties of selected examples of artefacts for X-ray CT are reported in Table 3.

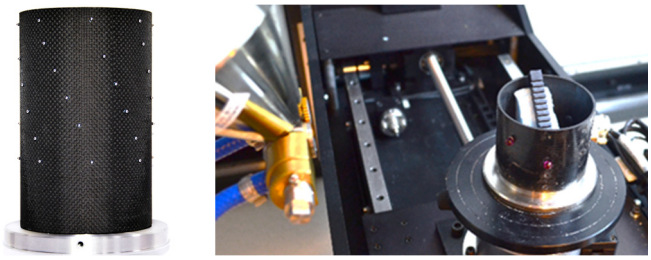

Figure 25. Left: "Carbon tube" artefact (University of Padova) for CT systems geometry calibration [76]. Right: "CT tube" (DTU) positioned on a CT scanner rotary table with a miniature step gauge placed inside [271].

Table 3.
Selected examples of dimensional artefacts for CT; L is the maximum edge length and U is the expanded calibration uncertainty (k = 2) [271].

Artefacts (source)	L (mm)	U (µm)
Calotte cube (PTB [20])	10	1.0
Tetrahedron and *Pan Flute* (Univ. Padova [46])	25	1.6
CT ball plate (DTU [271])	40	1.7
Miniature step gauge (DTU [45])	42	1.7
CT tube (DTU [271])	60	2.2

Workpiece-like and dismountable artefacts

Several workpiece-like artefacts with complex geometries have been developed for task-specific applications, in order to test and calibrate measuring systems using geometries and materials that are as similar as possible to those of actual workpieces. Such workpiece-like artefacts are needed in particular when the substitution method is applied, with similarity conditions to be satisfied [152] [279]. In the case of X-ray CT, actual workpieces can include difficult-to-access or inner features (e.g. inner geometries or porosity) that are measurable by CT but not by optical or tactile measuring systems. To obtain workpiece-like artefacts with inner geometries that can be calibrated by tactile reference measurements, dismountable artefacts (i.e. artefacts that can be disassembled) have been developed. Figure 26 shows an example of a dismountable artefact produced by dividing a small aluminium cylinder head into four pieces (so that most inner surfaces can be reached with tactile probing) and adding reference geometries (spheres and cylinders) to define a coordinate system for aligning the measurements in the disassembled and re-assembled state [269]. Hermanek et al. [130] developed a dismountable cylindrical artefact with calibrated internal hemispherical artificial defects for achieving traceability of CT measurements of internal porosity (Figure 27). Experimental investigations demonstrated that by scanning the artefact together with the workpieces under investigation, it is possible to implement procedures that allow correction of systematic errors in porosity measurement results by optimising the parameters used for the evaluation of the acquired data [132].

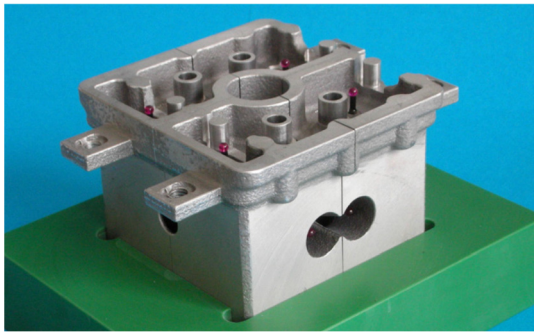

Figure 26. "Mini-Cylinder Head" dismountable artefact (workpiece-like artefact), composed of four segments on a holding plate; ruby spheres used for alignment are visible on the top plane of the artefact [23].

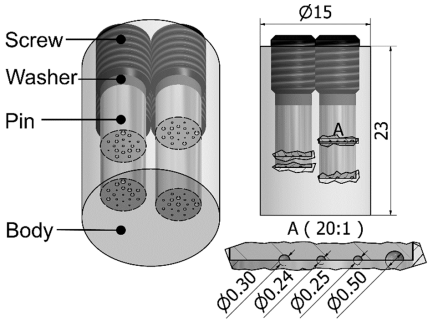

Figure 27. Dismountable artefact with calibrated artificial defects for achieving traceability of CT dimensional measurements of internal porosity [131]. Dimensions are reported in millimetres.

Artefacts for large-scale metrology

Large-scale coordinate metrology deals with coordinate measurement tasks for objects in which the linear dimensions vary from one metre to hundreds of metres [86] [258]. Calibration of large-scale measuring systems may require large artefacts. Large workpiece-like artefacts would have the advantage that almost all significant error influences (such as temperature, gravity, clamping and measuring strategies) can be kept very similar, which implies that systematic errors can be determined and corrected in a comparatively simple way. However, due to the high costs and small part numbers in large-scale manufacturing, the use of large workpiece-like artefacts cannot be always economically feasible. More often, large-scale artefacts are realised by combining length artefacts. Figure 28 shows an example of an L-shaped dismountable artefact for large-scale metrology [268], which was supported by a multiple-point mounting based on a hydraulic system that minimises bending by providing the same force for every supporting point of the artefact (see Sect. 5 and Figure 43). Figure 29 shows the "PTB's reference wall" with rod-shaped artefacts of up to 12 m in length, which was set up for testing and calibrating mobile 3D large-scale measuring systems (Figure 29). The test lengths are realised using thermally stable carbon fibre reinforced material and mounted on the wall, free of strain. The expanded measurement uncertainty (k = 2) of the different embodied test lengths is less than 5 µm.

In general, high geometric accuracy and stability of length artefacts can only be realised over lengths up to a few metres. To overcome this limitation in testing large-scale CMSs, the latest revision of ISO 10360-2 allows interferometers to be used as virtual length artefacts [147]. A review of calibration methods and

adopted reference artefacts for large-scale measuring systems is reported elsewhere [95]. In addition to classical monolithic measuring systems, modern large-scale measuring systems are constituted by constellations of sensors, allowing greater flexibility, scalability and portability, as well as a general reduction of costs [99]. A manufactured artefact made up by a series of infrared reflective spheres, for calibrating a mobile spatial CMS was presented by Galetto et al. [98]. A cooperative approach relying on the combination of angular and distance measurements yielded by sensors of several large-volume metrology systems, using a calibrated scale bar with reference points is presented elsewhere [97].

Figure 28. L-shaped dismountable artefact for large-scale metrology developed within the MESTRAL project [268].

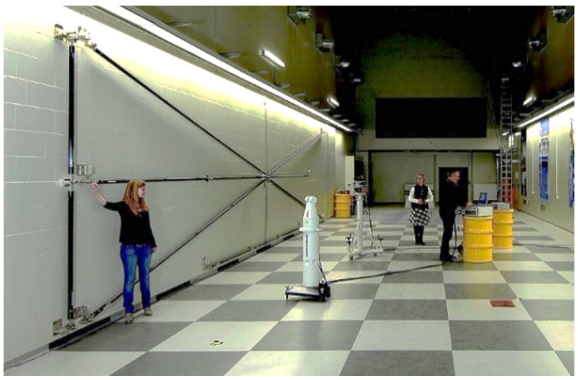

Figure 29. PTB's reference wall for testing and calibrating mobile 3D measuring systems for large measuring ranges up to 12 m (source: PTB).

Artefacts for micro- and nanometrology

Specific artefacts have been developed for micro- and nanometrology, and particularly for testing and calibration of micro-CMSs. In addition to miniaturised artefacts developed for downscaling geometries and test procedures of classical coordinate metrology, task-specific artefacts were realised to measure sensor-specific characteristics, such as force-induced deformations for tactile microprobes or minimum structure sizes that can be measured with non-contact sensors. Reviews of available artefacts for contact and non-contact probing systems at micro- and nano-scales are reported in [218], [217] and [59]. In the following, examples of 3D micro- and nano-artefacts are mentioned, without aiming to be exhaustive: many more artefacts exist as documented in the above reviews.

Several artefacts based on 3D-structures representing multistep pyramids have been developed, with micro- and nano-dimensions. Figure 30 reports a 3D pyramidal measurement standard developed by PTB, in which the terraces of the pyramids and the substrate are patterned with so-called nanomarkers, whose centres serve as 3D-reference points [243]. The pyramids consist of platinum, being patterned onto the substrate using the focussed ion beam (FIB) method (which was subsequently used to write also the ring-shaped nanomarkers). Using this artefact, not only the calibration factors for the three scan axes, but also the crosstalk between them can be determined. For the case shown in Figure 30, the size of the 3D-pyramids were chosen to fit the 3D measurement volume of most common SPMs. Other artefacts with similar 3D pyramidal geometries were developed on larger scales, with dimensions up to the millimetre-range, targeting to close the gap between nano- and macro-scale artefacts, for their use with instruments other than SPMs, such as stereophotogrammetric SEM, confocal laser scanning microscopes, and optical CMSs. For example, Dai et al. [66] developed an artefact including several inverse pyramids, each having dimensions of 6.5 mm × 6.5 mm × 1.5 mm, allowing the characterization of micro/nano-CMMs with measurement volumes of a few cubic centimetres. Galantucci et al. [96] developed pyramidal artefacts, including sub-millimetre and freeform features, for characterising and calibrating measuring systems based on stereo-photogrammetry, for applications such as measurement of 3D printed microfluidic devices [117] and microgears [229].

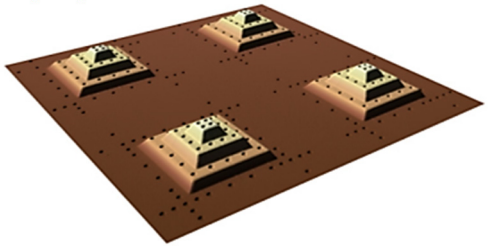

Figure 30. Geometry of the PTB's 3D pyramidal measurement standard measured by a SPM [243]. The image size is 84 µm x 84 µm, while the single pyramids have base line of approx. 20 µm and height of approx. 3 µm.

A multiple height artefact for calibration of the height response in 3D microscopy was developed by De Chiffre et al. [67]. The artefact comprises multiple steps having a common vertical axis and is suitable for transferring height traceability to 3D techniques at the micro- and nano-scale, including 3D SEM [44]. Similar multiple height artefacts were developed for testing and calibration of other 3D measuring systems [183]. As discussed in Sect. 2, the available artefacts with the smallest steps are single crystals with monoatomic steps (see Figure 6).

A "micro contour" measurement standard was produced by PTB (Figure 31) by wire electro-discharge machining, obtaining surfaces which are well suited also for optical measurements. A range of details and features present on the measurement standard, including sloped surfaces, allows several parameters of the measuring instrument to be studied [216]. Its design derives from the guidelines on acceptance and reverification testing of contour measuring systems according to the tactile stylus method, but has been miniaturised and modified for use in conjunction with several microsensor applications.

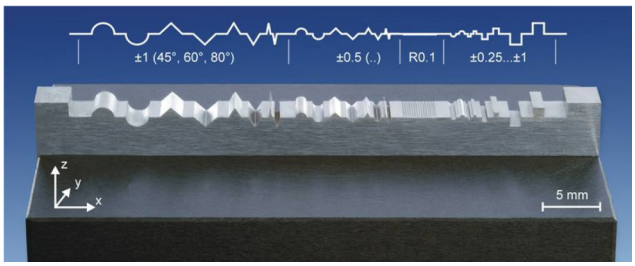

Figure 31. "Micro contour" measurement standard [216].

When measuring micro-features with high aspect ratio, specific measurement procedures and artefacts are requested. An example is the "fibre gauge" shown in Figure 32, consisting of a set of optical fibres protruding from a flat surface [202]. The fibres are arranged as a regular array of different height cylinders, with aspect ratios up to 20:1. The fibre gauge can be applied to calibration of the

height response of most contact or non-contact measuring systems for 3D metrology at microscale. The exemplar shown in Figure 32 includes high aspect ratio holes as well, which are specifically useful for error characterisation in micro-CT [49]. Other artefacts with micro-features are also required for testing specific characteristics of CMSs, such as the metrological structural resolution [8] [50] [138] [295].

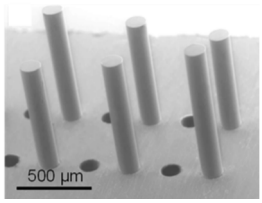

Figure 32. SEM image of the "fibre gauge" featuring fibres and holes with high aspect ratio [202].

Finally, it is noted that, since current micro-CMMs can reach maximum permissible errors of length measurement ($E_{L,MPE}$) of 250 nm or less, it is requested that artefacts for micro-CMMs testing and calibration should be calibrated to uncertainties better than 50 nm. However, such calibration uncertainty is too small for most 3D artefacts (see Table 4); for example, the calibration of ball plates and 3D artefacts based on spheres to uncertainties below 100 nm is difficult and tends to rely on other tactile micro-CMMs [59]. As a consequence, micro-CMM testing and calibration often have to rely on time-consuming measurements using gauge blocks, and the reached $E_{L,MPE}$ values can be higher than what would actually be possible [59]. Future developments are needed to reach 3D artefacts with reduced calibration uncertainties.

3.4. Angle

The coherent unit for plane angles is the radian, which is a dimensionless derived unit of the SI; in fact, it corresponds to the ratio of two lengths [31]. Hence, angle metrology is considered part of length metrology [27]. Angle metrology plays a decisive role in advanced manufacturing, e.g. for controlling the rotational deviations of moving axes, which is critical for the achievable manufacturing accuracy of machine tools [105]. Moreover, the angular orientation of rotary axes in multi-axes machines needs to be measured, adjusted and monitored.

Angular encoders are measuring systems for determination of angular positions over 360°. Their operation is based on the use of a circular grating, which has been patterned on a substrate and whose angular displacements are probed by one or more reading heads using an optical or magnetic signal; see Figure 33. Depending on the type of grating and the processing of the measurement signals, the types of encoders are either relative (using uniform gratings) or absolute (using Gray-code type gratings) angle measuring systems.

All angle measuring instruments and angular artefacts extending over the full circular range of 360° can be calibrated by self-calibration techniques [91] using the inherent property of the full circle: that all individual angular deviations sum up to zero over 360° (2π rad periodicity). A high-precision angle comparator based on two independent angular gratings allowing for application of different self-calibration approaches has been described by the PTB [236]; an updated report on the achieved level of self-calibration was given in [111]. A comparison of a rotary encoder used as a transfer measurement standard was reported [168], while a calibration guideline for angular encoders has recently been published by EURAMET [89]. The National Metrology Institute of Japan also used self-calibration approaches for precision calibration of angular encoders [281] [282].

Mirror polygons are angular artefacts extending over 360°. They, however, realise angles at a limited number of angular positions only, usually regularly distributed over 360°. Examples are polygons with 6, 12 or 24 flat faces, which are often used (see Figure 34). The mirror polygons are made of quartz glass, or glass ceramics with low CTE, such as Zerodur, or from metal, such as tungsten or chrome carbide. The quality of the mirror polygon is dependent on the achieved flatness of the mirror faces and their relative misalignment, expressed as pyramidal error. Often, polygons are used with a housing providing defined apertures to measure the angular direction of the mirror surfaces. The result of the latest international comparison of NMIs on a mirror polygon were reported in [174]; the measurement uncertainties of the participants varied from 8 to 100 milli-arcseconds (k = 1). A different artefact related to the polygon is the so-called reflecting cube, which has up to six orthogonal optically-flat faces (typically square to 1 arcsecond), and is used with autocollimators or interferometers to establish perpendicularity in in three mutually orthogonal directions.

Figure 33. Angular grating with 400 mm diameter consisting of 2^{17} = 131 072 graduation lines resulting in angular intervals between adjacent lines of 9.89 arcsec and one reading head being the core components of an angular encoder (source: EURAMET).

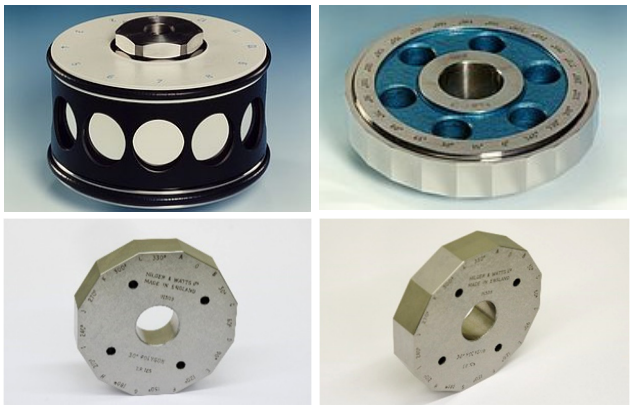

Figure 34. Photos of mirror polygons. Top left: 12-sided polygon with housing and aperture holes (source: PTB). Top right: 24-sided polygon (source: PTB). Bottom: 12-sided polygon (source: H. Haitjema, KU Leuven).

90° standards are important references for alignment of motion axes of machine tools and measuring instruments. They are often made from granite (or ceramics), and are available in square, rectangular or triangular shape and in different sizes. The quality of the polished surfaces also allows 90° standards to be used as straightness measurement standards, see Sect. 3.2.

Linear and angular gauge blocks are still used routinely to realise angles. Linear gauge blocks can be used in combination with sine plates [211]. In analogy to linear gauge blocks, which can be wrung together to realise arbitrary lengths (see Sect. 3.1), angular gauge blocks can also be wrung to realise arbitrary angles. If the wringing process is performed correctly, it introduces no significant uncertainty contributions, because the surfaces of the angle gauge blocks are strongly held together by molecular forces. Similar to linear gauge blocks, angle gauge blocks are made of steel, tungsten carbide or ceramics. Figure 35 shows a set of angle gauge blocks.

Figure 35. Set of angle gauge blocks (source: PTB).

Another passive method of generating angles with typical uncertainties of 0.1 arcsecond is through indexing tables based on Hirth couplings (mating face gears) which exploit the principle of elastic averaging [211] to provide indexing accuracies better than the spacing errors of the engaging gear teeth. These tables are extensively used in the optics industry for measuring critical angles and for calibrating rotary tables (see e.g. [211]).

The most stringent requirements on small angle metrology using electronic autocollimators today result from basic research. Autocollimators with only millimetre-sized apertures play an important role in laterally high resolving deflectometric measuring instruments for surface characterization of beam deflecting optics in synchrotron radiation and free-electron laser facilities [237]. It should be noted that in most deflectometric measuring instruments, another type of angular artefact also plays an important role as an optical element, namely the pentaprism. Pentaprisms always reflect an optical beam by 90°, independent of small angular deviations of the incoming beam or small angular deviations of a linear movement of the pentaprism. An international comparison using an electronic autocollimator has recently been finished [112]. During the comparison, the influence of atmospheric pressure deviations on the measurement results of autocollimators was analysed [113]. The results of a recently finished European joint research project on angle metrology were published in [293]. A new instrument (SAAC: solid angle autocollimator calibrator) was described, which allows the calibration of the *x*- and *y*-components of spatial angles simultaneously with expanded uncertainties of 0.015" and for different distances between the device under test (autocollimator) and the SAAC between 250 mm to 1.8 m [261].

3D angle artefacts are used for production quality control of taper roller bearings. For example, a 3D angle artefact was developed to maintain the traceability of 3D angle measurement from NIST to various products based on the substitution method per ISO 15530-3 [152]. The material of this artefact is AISI 06 steel, manufactured to a hardness within the range of 58 to 62 (Rockwell). The surface texture of this artefact is controlled to be no more than 0.2 µm (*Ra*). Two conical angles (denoted by Angle A and Angle B) are incorporated into this artefact, as shown in Figure 36, with the nominal half angle value of 20° and 10° respectively. This artefact was calibrated on a precision CMM at NIST, achieving an expanded calibration uncertainty ($k = 2$) of 0.000205° (which is approximately 0.7") for both angles.

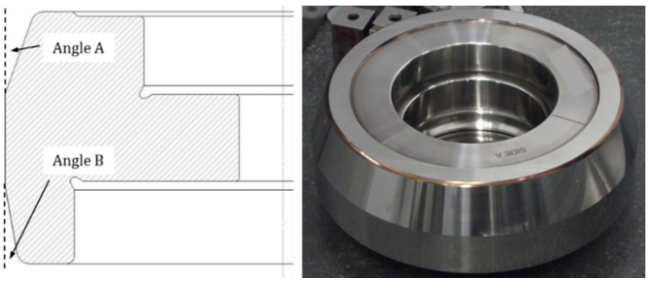

Figure 36. Artefact for 3D taper angle metrology (source: Timken).

4. Availability of dimensional artefacts

The available dimensional artefacts and their main characteristics were presented in Sect. 3. The ranges covered by existing dimensional artefacts as well as the uncovered ranges can be analysed, with indication of needs for new artefacts, following an approach used in [70], [120], [253] and [68]. In this section, the availability of artefacts is briefly discussed with respect to dimensions and measurement uncertainty, considering by way of example the main areas of surface metrology and coordinate metrology (particularly for freeform and micro-scale applications). Also, the availability of dimensional artefacts for the establishment of traceability directly in the production environment is discussed.

Surface metrology

The present situation concerning surface metrology (see Sect. 3.2) can be illustrated with respect to the traceability of surface texture measurements: Figure 37 shows the range of different measuring instruments including an indication of existing dimensional artefacts in a Stedman-like diagram [270]; here, only dimensions are shown while the diagram shows no information about geometrical complexity. Comparing the present measurement possibilities with requirements from production, it is quite clear that relatively large areas of the diagram are uncovered, indicating the need for dimensional artefacts. Besides, all measurement standards represent low aspect ratios and no real 3D measurement standards are available in this area. As discussed in [120], new measurement standards for surface texture made out of glass, ceramics and metals, as well as inorganic materials, are needed.

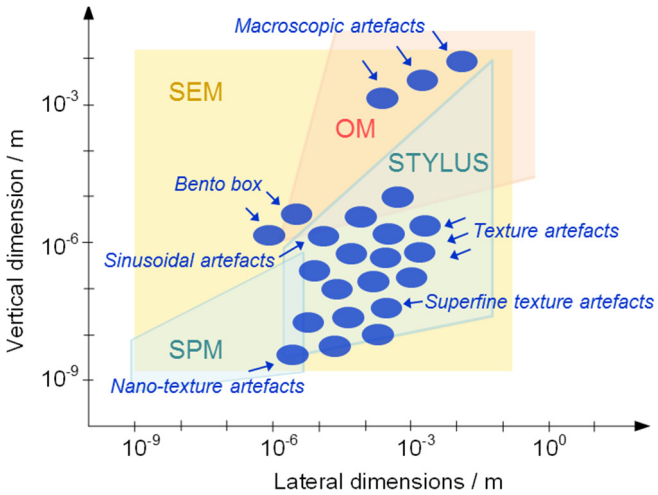

Figure 37. Measuring instruments and dimensional artefacts (in blue) for surface texture measurements. Adapted and updated after [70] and [120].

Freeform metrology

Freeform surfaces are a large industrial area representing challenging measurement tasks, and the underlying manufacturing technology relies to a large extent on the capabilities of the metrological set-up that will deliver data from the product or process to stabilise production. A classification based on freeform part dimensions, shape complexity, material, surface and tolerances has been produced in [253]. Task-specific methods for performance evaluation of measurement systems and for the evaluation of measurement uncertainty can rely on dimensional artefacts having freeform geometry (see Sect. 3.3). Figure 38 is adapted and updated from [253] and shows dimensions and calibration uncertainty of some examples of freeform artefacts.

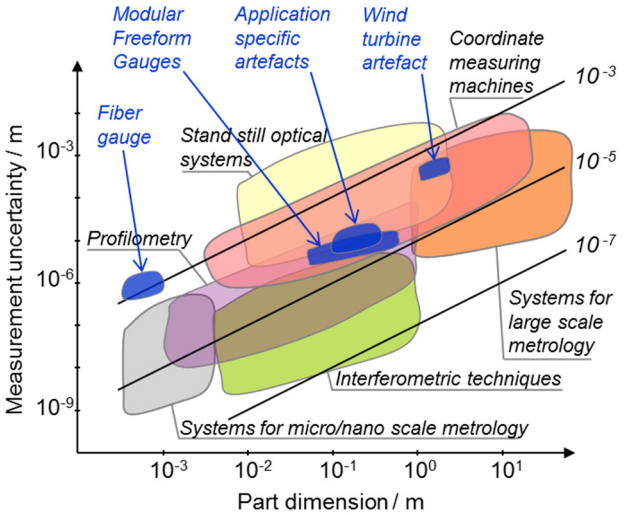

Figure 38. Typical range of measurement uncertainty vs. part dimension for different categories of measurement systems along with dimensions and calibration uncertainty of some examples of freeform artefacts (in blue). Adapted and updated after [253] and [199].

Micro-coordinate metrology

Micro-CMMs are now of interest because of their ability to perform geometrical measurements in three dimensions to high accuracy with low uncertainties. Claverley and Leach [59] have provided a review of available artefacts for micro-CMMs, concluding that often micro-CMMs cannot yet be verified in accordance with existing specification standards, and suggesting actions for future standardisation work required to rectify these issues. In the same review, the available artefacts are also classified as shown in Table 4, according to several features: their fitness as a calibrated test length with 1D, 2D or other calibrated measurands, their suitability for use with other systems beyond contacting micro-CMMs (such as optical and video CMSs), and their geometry, which determines their ease of use, their limitation and their suitability for use with reversal algorithms, and their calibration uncertainty (although for several artefacts this value is not reported).

Table 4.
Examples of available artefacts for micro-CMMs; calibration uncertainties (U_{cal}) are expressed in nanometres [59].

Artefacts	1D	2D	Other	Tactile	Optical	Video	Reversal	U_{cal}	Ref.
Gauge blocks	X			X				30	[215]
METAS miniature ball bars	X			X				50	[177]
A*STAR mini sphere beam	X			X				65	[53]
Sandia silicon 1D standard	X			X		X		400	[278]
Zeiss miniature ball plate		X		X			X	110	[214]
PTB micro-ball plate – smooth		X		X					[82]
PTB micro-ball plate – rough		X		X	X				[82]
METAS ball plate		X		X			X		[177]
Kruger ball plate		X		X			X		[175]
Kruger cylinder plate		X		X	X	X			[175]
Kruger hole plate		X		X	X	X	X		[175]
Sandia silicon 2D standard		X		X		X		400	[265]
3D Calotte cube			X	X				1000	[20]
PTB micro-hole standard			X	X					[218]
Polytec step height standard	X		X	X	X			450	[34]
PTB micro-tetrahedron			X	X					[176]
Calotte plate		X	X	X				1500	[22]
PTB micro-contour standard	X		X	X	X				[216]
Pyramidal standard		X	X	X					[61]

Production-integrated measurements

In order to address constantly increasing needs in advanced manufacturing, it is often necessary to integrate measurements directly in the production (see Sect. 1). Figure 39 illustrates an example of calibrated master shaft for process control in production using a measurement system by Marposs [204]. Figure 40 shows process control in production using a CNC comparator by Renishaw, based on the comparison of production parts to a reference master part, which compensates for changes in the thermal conditions of a shop-floor environment, and is intended for factories with wide temperature variations [241]. Applying an approach with the simultaneous measurement of part dimension and temperature over time (dynamically), supported by modelling of the thermo-mechanical effects, the corrected length at 20 °C and its measurement uncertainty can be predicted with a sub-micrometre uncertainty within 10 minutes after machining [69]. Probe zeroing for dynamic length measurement (DLM) under production conditions is shown in Figure 41.

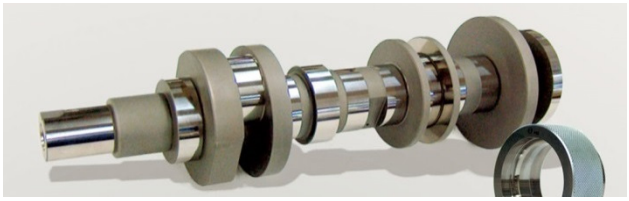

Figure 39. Calibrated master duplicating the manufactured part and used for the zero-setting of measuring instruments with electronic sensors or dial gauges (source: Marposs).

Figure 40. Master for process control in the production using a CNC gauge by Renishaw (source: DTU).

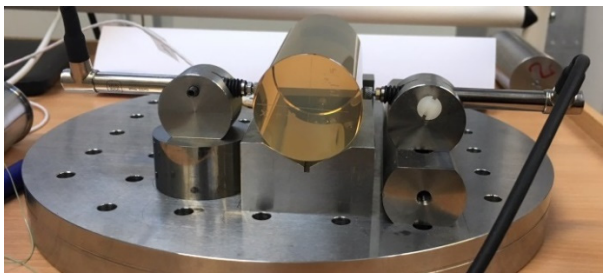

Figure 41. Probe zeroing for DLM in the production of ø40 mm turned parts (source: DTU).

5. Guidelines for development of dimensional artefacts

From the sections above, it can be concluded that there is a large number of artefact types used for dimensional metrology, and this number is still growing. Whilst the specific artefact is designed to meet a specific function, there are a number of general artefact design considerations that can be discussed. The first place to start when designing an artefact, is to consider exactly what its function will be: what is the primary measurand, are there other measurands, what measuring instruments will it be used with and

which specification standards will it address? For example, in the case of a flat reference, the primary measurand is flatness, other measurands may be straightness, the measuring instrument for which it will be used may be contact CMS and the specification standard will be ISO 12781-1 [151] (and maybe also ISO 12780-1 [150]). The key requirements for realising unambiguous measurands were covered in the introductive part of Sect. 3.1 (including the definitions of reference points, alignment, and origin). The differences between unidirectional and bidirectional measurands were examined in Sect. 2 (see Figure 5). Another important design requirement is how the artefact will be mounted and aligned (see below). Once these top-level design requirements have been identified, the detailed requirements must be considered. As with any precision design, the principle of reduction should be applied wherever possible. Replacement of complex assemblies (e.g., an artefact with several DOF of alignment motion) with fewer components will always simplify analysis [191]. Fewer components will almost always lead to less tolerance stack-up. When there are competing solutions to the artefact design, each of which satisfies the requirements of comparable cost and performance, it is best to choose the simplest (a principle often referred to as Occam's razor [191]). Once the above questions (function, measurands, measuring instruments and specification standards) have been addressed, the artefact can be designed. The key issues to consider include many of the following.

Stiffness

Artefacts are usually required to be rigid, to preserve the calibrated values over time and specifically at time of use. Typical deforming forces are gravity, fixturing forces and measuring forces; typical countermeasures to minimise their effects are proper design of the artefact layout and of the supports for fixturing, and careful choice of the material. The deforming forces are briefly overviewed below, while the possible countermeasures will be covered subsequently in specific clauses.

Gravity is unavoidable and may or may not be an issue depending on the intended application. In all cases, as deformation is a high order function of the artefact size (second to fourth order in most cases), this problem is relevant for medium to large sized artefacts, while usually negligible for medium to small sizes. Due to the high repeatability of deadweight deformations, in principle they can be overcome easily by ensuring that the fixturing and the orientation to the gravity vector are the same in calibration as in use. For some artefacts, the conditions at calibration are specified; e.g., for gauge blocks, ISO 3650 [144] prescribes orientation and rest points for either short (≤ 100 mm) or long (> 100 mm) gauge blocks. However, standardising the conditions at use is difficult or impossible. Even in the example case of gauge blocks, their use, e.g., in CMM performance verification [147] includes multiple orientations to the gravity vector. The general rule applies that all GPS specifications hold in the absence of gravity by default, unless otherwise specified (ISO 8015 [146]). Special care is then required for medium to large artefacts when they are intended in multiple orientations or, more generally, when the calibration cannot occur at the same conditions as in use.

Fixturing forces are generated when mounting the artefact onto the instrument base to allow measurement (see below for further discussion of the design aspects for supports for fixturing). The purpose of fixturing is to ensure that the artefact does not move relative to the measuring instrument during the measurement. The degree of fixturing should match the expected displacing forces, i.e. measuring forces (typically for contacting instruments) and inertial forces (for moving table instruments). The artefact mass is usually beneficial, as the friction at the resting points may be high enough to counteract the measuring forces. However, mass is of little help for inertial forces (if any), as both the counteracting friction and the inertial force are proportional to the same artefact mass.

Measuring forces are induced by probing. The obvious case is that of contact probing: in spite of the many possible designs [283], all contact probing methods need a force to react to, which is generated by contact and balanced by an opposite force on the artefact. Probing forces are unavoidable; even probing systems specifically designed to minimise this force (e.g., [126], [133], [58]) cannot completely eliminate it. Probing forces are virtually eliminated with non-contact probing systems, such as optical probes [284]; in this case, the measuring force usually generates a negligible effect.

Design of the artefact layout

The deforming forces are predictable to some extent, and proper design of the artefact can minimise the deformation. Probably the most severe deformation for many artefacts is bending, particularly for large artefacts. Given a certain amount of deformation, the artefacts of form are almost immediately impacted in their metrological characteristic, and there is little margin to mitigate the effect. For example, the reference face of a straightedge can be designed to be vertical, so that the horizontal measuring lines are unaffected by gravity; however, this may not always be possible, i.e. when the desired straightness plane ([150], Sect. 3.1.3) is vertical. The straightedge can also be ground with the reference plane horizontal and mounted according to the future application. The effect on measurement standards of size can be reduced to virtually zero by aligning all reference elements to the artefact neutral axis or plane. This is the case e.g., for gauge blocks [144], most step gauges and ball/hole plates (Figure 42). The effect of compression/tension is usually unavoidable. For example, considering a simple gauge block in the vertical orientation, it will be under compression if resting on its lower face, or under tension if hanging from its upper face, or neutral on average if supported at its midpoint. In general, the elongation/compression of a vertical gauge block is $\left(L_{\mathrm{a}}^2 - L_{\mathrm{b}}^2\right) g/(2E_s)$, where L_{a} and L_{b} are the gauge length above and below a resting point respectively, g is the local acceleration due to gravity and E_s is the specific elastic modulus of the material (see also below in the clause on materials choice). The horizontal cross section does not appear in the above equation; increasing the dimension – making the artefact heavy and apparently stiffer – does not help. The compression/tension due to deadweight is usually negligible, but for long and accurate vertical artefacts it may be significant; e.g., 0.18 µm for a 1000 mm steel gauge block resting on its measuring face.

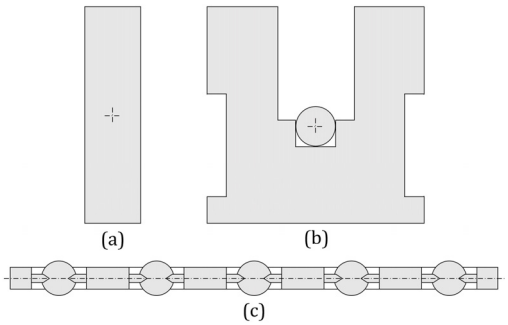

Figure 42. Cross section of (a) a gauge block, (b) a step gauge, and (c) a ball plate. The measurand line (or plane) lays on the neutral axis (or plane).

Design of the supports for fixturing

The most common method applied for mounting artefacts onto a support structure is kinematic mounting [191]. The most used mounts are the three-vee (Maxwell coupling) and the tetrahedron-vee-flat (Kelvin coupling), holding a counterpart with three matching spheres, and the three cylinders onto

corresponding sphere pairs [284]. These mounts implement the concept of point-contact constraint: three in a tetrahedron, two in a vee and one on a flat for a sphere; two on a sphere pair for a cylinder. The load can be provided either by gravity or by springs (preload). Often the contact points for a mounting arrangement are chosen so as to minimise undesired dimensional changes in the artefact. Two well-known examples when mounting length artefacts horizontally are the Airy points for long gauge blocks (zero slope at ends, distance of $L/\sqrt{3} \approx 0.577\,L$ between symmetrical rest points) [144], and the Bessel points for line scales and straightedges (minimum straightness, distance of $0.559\,L$ between symmetrical rest points) [221].

When an artefact is designed to be fixtured, proper design would drive the inevitable stress flow (from the fixturing to the rest points) along a path in the material with minimum involvement of the metrological characteristic, to maximise decoupling. For example, areas of the artefact designated to hold the fixturing can be laid out close to, and in correspondence with, the resting points, thus confining the deformation to local compression only with no or little overall bending. Extra material can be added nearby to increase the local stiffness.

For large and not very rigid artefacts, kinematic mounts may be inadequate and over-constraining supports may be necessary. In this case, careful attention should be paid to ensure that the same resting conditions at calibration will be matched in future use; even microscopic changes of the relative position of the multiple resting points can result in significant changes of load distribution, potentially altering the artefact metrological characteristics. When a single permanent piece of resting equipment is not feasible (e.g., because disassembly is required), then some self-balancing device is recommended. Examples are passive hydraulic systems: each contact is made of a plunger sliding in a chamber with a fluid, all chambers are connected to each other, and the plungers self-align to the gravity vector (see Figure 43, which refers to the case of the large-scale artefact shown in Figure 28).

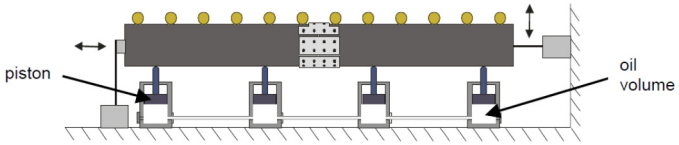

Figure 43. Scheme of a hydraulic mounting system [19].

Fastening and fixing

Many dimensional artefacts are often a combination of objects that need to be assembled during manufacture or prior to use. The artefact in Figure 44, for example, has several carbon fibre rods connected by machined steel end-pieces, to which ceramic spheres are connected. The manner in which one part of the artefact is connected to another is often critical to the operation of the artefact. Common methods are the use of fixings and adhesives, but care must be taken to avoid significant over-constraint (often leading to internal stress and dimensional changes), and mismatched thermal expansion and/or elastic properties. A thorough discussion of fastening and fixing in precision engineering applications is given elsewhere [41].

Choice of the material

An artefact must have a predetermined degree of mechanical stability when mounted for measurement (and possibly also when stored and/or transported to avoid permanent distortion). The mechanical properties, such as Young's modulus, Poisson's ratio and hardness, of the artefact material must be such that it does not damage during use, for example when measuring with a mechanical CMS probe. Metals are probably the most utilised material due to their high strength, ease of machining and relatively low CTE, but they can have relatively high mass and poor corrosion properties. Many metal and ceramic materials are heat treated to stabilise their properties. Ceramic and glass materials (and their hybrids) can have beneficial mechanical and thermal properties but are brittle, so mechanical shocks need to be avoided. Carbon fibre is a high-strength, low-mass material that is often used as the frame material for artefacts (see examples in [3] and Figure 44). Carbon fibre reinforced materials and other materials with low X-ray attenuation coefficient are useful for developing artefacts for X-ray CT measuring systems (see Sect. 3.3). There have been some steps in the direction of polymer artefacts, mainly for X-ray CT and due to their potential for cost effectiveness, but issues with dimensional stability are under investigation (see e.g. [6], [206]). In some nanoscale applications, the self-ordering nature of biological molecules has been exploited (see Sect. 2), although there are disadvantages with stability [25]. Many of the materials issues discussed in this section are reviewed elsewhere [57]. Materials are stressed by the force due to gravity proportionally to their density ρ, and are strained inverse proportionally to their elastic modulus E. Effectively, the specific elastic modulus $E_s = E/\rho$ is of interest for minimising the deadweight deformation [19]. Table 5 compares different materials, and shows that most materials – including most metals – have similar specific elastic moduli, while special carbon fibres exhibit interesting values, twice those of ceramics such as alumina and seven times those of metals such as steel and aluminium. In spite of its interesting performance, carbon fibre may exhibit sensitivity to humidity [230]. Carbon fibre-reinforced polymers also exhibit secular drift, mainly due to its epoxy content, and can have CTE that vary considerably in orthogonal directions. The magnitude of such effects greatly depends on the lamination process.

Figure 44. Ball tetrahedron artefact (source: Trapet Precision Engineering).

Table 5.
Specific elastic modulus (E_s) of selected materials.

Material	E (GPa)	ρ (kg/dm^3)	$E_s = E/\rho$ (m^2/ms^2)	
Carbon fibre, special	600	3.2	190	190
Alumina	350	3.8	92	92
Carbon fibre, common	90	1.6	56	56
Steel	210	7.8	27	27
Aluminium	69	2.7	26	26
Titanium	110	4.5	24	24
Granite	52	2.5	21	21
Nickel	170	8.9	19	19
Cast iron	130	7.2	18	18
Pine wood	9	0.5	18	18
Oak wood	11	0.75	15	15
Copper	120	8.5	14	14

Thermal stability

The thermal stability of a dimensional artefact is often one of the most important properties; increasingly so as the size of the

artefact increases. The thermal disturbance to a dimensional artefact stability is mostly due to expansion caused by temperature changes and temperature gradients. These changes can arise from many sources, such as environmental changes, localised internal heat sources (although unlikely with passive artefacts) or the operator's hand. Some effects may be virtually unchanging or tending only to slow change, while others may be one-off or repeating transients. Therefore, when considering the effect of temperature on the design and operation of a dimensional artefact, static, quasi-static and dynamic behaviour needs to be considered.

Thermal expansion is a key materials property, but other thermal properties may be important, including conductivity, specific heat and diffusivity. Many of these design issues are discussed in depth elsewhere [57], where property groups are presented for various materials used for dimensional artefacts. Thermal effects are often found to be a dominant factor when considering the achievable measurement uncertainty with a given artefact. Relatively standardised methods exist for dealing with this influence factor [262] [153].

Surface properties

Surface properties, such as texture, chemistry, grain structure and the presence of coatings (designed or contaminant), can play a highly dominant role in artefact design. Whilst there has been significant research effort to model the surface interaction of a contact stylus during a measurement (see references in [190]), the effect of surface properties on an optical measurement is far more complex, and still an active area of research at all scales [185] [190] [228]. Also, different optical instrument modalities are better suited to different surface types. For example, fringe projection is more suited to a diffusely reflecting surface and deflectometry to a specularly reflecting surface [127]. Often, coatings can be applied to an artefact surface to facilitate a specific type of measurement, e.g. the use of Lambertian coatings for fringe projection on smooth surfaces. However, the effects of such coatings on the resulting measurement uncertainty need to be quantified [225]. There has been some work to produce spherical artefacts with well-controlled surface types for various applications (e.g. [169], [275]) and limited work to develop artefacts to try to verify the effect of different surface types on optical instruments (e.g. [118], [80]). More research is needed in this area before rigorous methods for calibration of optical methods can be standardised. Translucency can also have an effect on optical measurements, especially with ceramic or polymer materials. Surface (and material) properties can be problematic with X-ray CT measurement, especially where surface determination is key to the desired measurand [4] [21]. As schematically shown in Figure 45, different measurement techniques may produce different measurement results, depending on surface properties and measurement principle.

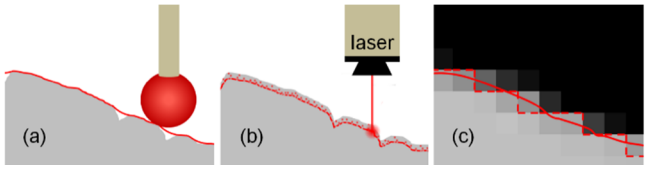

Figure 45. Different measurement techniques producing different measurement results: schematic representation of (a) tactile, (b) optical and (c) X-ray CT scanning of a surface. Red lines represent extracted points on the measured surface [51].

Optical properties

When an artefact is designed to be used with an optical instrument, the optical properties of the artefact need to be considered. Surface topography effects and translucency were discussed above, but the optical constants (refractive and absorption indices) for a material can have a relatively large effect on how light is reflected and/or transmitted at an interface/surface. Due to the required continuity of the electromagnetic field at an interface, there are phase changes that make the field appear to come from above or below the interface. These are well-documented effects, especially in the field of gauge block measurement (e.g. [196], [184], [277]). In principle, the effect can be calculated if the optical constants are well known, and corrected if the surface is of a single material. However, experience shows that prediction is not accurate enough and specific experimental investigation is usually carried out (e.g., the so-called "stack method" to measure the phase shift at the surface [186]). In all cases, the uncertainty of the correction must be accounted for (see e.g., [74]).

Storage, cleaning and handling

Calibration artefacts are costly and delicate items that must always be treated with care. Often, they are stored in sturdy boxes or storage drawers, sometimes with controlled and/or monitored environments (e.g., with temperature and humidity control and/or data logging). Packing materials must be considered with care: when optical quality surfaces are required, the surfaces should not be contacted in any manner, and dedicated mechanical packing solutions need to be used (e.g., polymer spring clamps that avoid the active surfaces). When storage is required without the need for transport outdoors, a simple low-surface energy polymer box (e.g., polypropylene) can be used with a lint-free filter paper base. Keeping artefacts clean and free from dust is often critical to their performance. However, cleaning should be kept to a minimum as there is always some change in the artefact as a result of the cleaning process [24]. Many different cleaning processes have been developed for dimensional artefacts; treating all artefacts as if they were optical surfaces is good practice. Their cleaning, storage and handling are covered in detail elsewhere [257].

Design for manufacture and metrology

When designing any precision engineered product, it is essential to ask the simple question: can the object be manufactured at a reasonable cost? This seemingly obvious question can save a great deal of re-design later in the manufacturing stage. To address the question at the design phase, the geometry, materials, available production systems, assembly and inspection must be considered. Questions to consider include: how will they be used (measured), where will datums and other reference features be placed, how long will the subsequent measurement process take, can reversal methods be used with the artefact [91] [93], and can more than one measurement modality be used with the artefacts (e.g., tactile and optical instruments [121])? The high level of design freedom offered by AM, for example, should encourage the designers to keep well in mind the design for metrology requirements; not just with dimensional artefacts, but also with actual products [244].

Another specific issue is the envisaged calibration method. Artefacts are usually recalibrated repeatedly over their life span, raising a technical as well as an economic issue. In principle, standard components such as gauge blocks, rings and plugs are most easily calibrated, as many primary [29] and secondary [137] laboratories provide the service. A design choice based on standard artefacts is desirable as far as possible. However, this may not always suit specific application requirements. When this is not possible, or when their assembly results in a non-standard layout (e.g., [247]), foreseeing (re)calibration is very important at the design stage. In some cases, specific features need to be added to ease the calibration – or even make it possible at all. A typical example is the addition of reference features (e.g., spheres) as datums to ease the alignment or the establishment of the artefact system of coordinates, e.g., for freeform artefacts (see Sect. 3.3). In some cases, specific auxiliary equipment or instruments may be

designed in combination with the artefact to address this issue (e.g., [19]).

6. Conclusion and outlook

This paper discussed the fundamental role of dimensional artefacts to support production by establishing the traceability of measurements. The main characteristics of the artefacts and their availability were examined. Numerous solutions were reviewed, ranging from standardised objects with simple geometry, such as gauge blocks, to new concepts, such as virtual calibration artefacts based on computer-generated holograms. In addition, guidelines were provided for the selection, use, and development of dimensional artefacts.

It is foreseen that the importance of metrological traceability and of confidence in the measurement results (expressed by the measurement uncertainty) will increase in future flexible manufacturing environments. The reason is that decisions in advanced manufacturing infrastructures, characterised by autonomous communication of machine tools and measuring instruments, require reliable information on the components to be produced through a series of subsequent process steps on different machines. Only if functionally relevant characteristics of components are measured traceably with stated uncertainties, can appropriate decisions be made on whether such components are within specification, and on whether proceeding either to the next machining step or to final assembly. Otherwise, undesired issues may occur, such as downtimes, disputes and product failure, with direct economic impact, and possible loss of reputation or legal repercussions.

The role of material artefacts remaining fundamental for establishing traceability in advanced manufacturing might seem contradictory compared to the recent revision of the SI, which eliminated material artefacts from the definitions of the measurement units. The definition of the unit of length is – and was even before the revision – based on the speed of light in vacuum, and the link to physical dimensions is carried out by interferometry, where the light wavelength is key. A practical problem is that usual ambient conditions affect the light behaviour and compensation for the air refractivity is required. This problem, together with the optical complications of interferometry, makes the direct interferometric linkage to the metre unpractical and/or not economical for industrial manufacturing in many cases. Thus, material artefacts continue to be essential intermediaries all along the traceability chain, form the SI unit definition to production control in manufacturing. It was shown that dimensional artefacts can not only compete in accuracy with direct interferometry, but can also be practical, robust, and fit for applications in harsh environments.

Some of the key issues for future research directions are summarised below. Concerning linear dimensions (see Sect. 3.1), the current calibration capabilities are limited by the detection of the artefact reference points for short lengths (e.g. in nanometrology) and from the thermal effects and air refractivity for long lengths (e.g. in large-scale metrology). Thermal issues are also often dominant in on-the-field applications and would benefit from improved materials and design for insensitivity. In the field of surface metrology (see Sect. 3.2), when measuring complex surfaces with high slope angles, there is still a need to establish methods and artefacts for the determination of the topography fidelity, which is a key requirement for future research. In coordinate metrology of complex shapes (see Sect. 3.3), several innovative solutions have been developed to establish traceability for specific cases. However, for some applications, such as in connection with AM parts containing hidden or internal features which are difficult to access and to emulate with artefacts, new task-specific solutions are under development and traceability challenges need to be solved. In addition, for micro- and large-scale coordinate metrology, future developments are needed to reach 3D solutions with reduced calibration uncertainties at acceptable costs. Finally, in angle metrology (see Sect. 3.4), when very demanding requirements are given for specific manufacturing control processes, such as very small angle measurement uncertainties or angle measurements on small surface areas, the use of product-like reference objects, calibrated by dedicated measuring instruments at NMIs, can be a viable approach.

Acknowledgements

The advice and comments from the CIRP STC-P officers and reviewers, as well as the fruitful discussions and suggestions from the colleagues in STC-P, are appreciated. Particular gratitude goes to the following persons who provided contributions and references: Vivek Badami (Zygo), James Claverley (NPL), Chris Evans (UNCC), Luigi Maria Galantucci (Politecnico di Bari), Maurizio Galetto (Politecnico di Torino), Wei Gao (Tohoku University), Benjamin Häfner (KIT), Han Haitjema (KU Leuven), Christopher Jones (NPL), Wolfgang Knapp (Engineering Office Dr. W. Knapp), Gisela Lanza (KIT), Michael Marxer (NTB), René Mayer (Polytechnique Montréal), Marcel Moghadam (DTU), Edward P. Morse (UNCC), Kang Ni (Timken), Danilo Quagliotti (DTU), Enrico Savio (Univ. Padova), Alan Wilson (NPL), Jose A. Yagüe-Fabra (Univ. Zaragoza), Filippo Zanini (Univ. Padova).

Certain commercial entities or products may be identified in this document, e.g. to describe concepts adequately. Such identification is not intended to imply recommendation or endorsement by the authors, nor to imply that the entities or products are necessarily the best available for the purpose.

References

[1] Abdelaty A, Walkov A, Franke P, Schödel R (2012) Challenges on double ended gauge block interferometry unveiled by the study of a prototype at PTB. Metrologia, 49(3):307-314.

[2] Aburayt A, Syam WP, Leach RK (2018) Lateral scale calibration for focus variation microscopy. Meas. Sci. Technol. 29:065012.

[3] Acko B, McCarthy M, Härtig F, Buchmeister B (2012) Standards for Testing Freeform Measurement Capability of Optical and Tactile Coordinate Measuring Machines. Meas. Sci. Technol. 23:094013.

[4] Aloisi V, Carmignato S (2016) Influence of Surface Roughness on X-ray Computed Tomography Dimensional Measurements of Additive Manufactured Parts. Case Studies in Nondestructive Testing and Evaluation, 6(B):104-110.

[5] Andreu V, Georgi B, Lettenbauer H, Yague JA (2009) Analysis of the error sources of a Computer Tomography Machine. Proc. Lamdamap conference 2009; 462-471.

[6] Angel J, De Chiffre L (2014) Comparison on Computed Tomography Using Industrial Items. CIRP Annals, 63:473-476.

[7] Angel J, De Chiffre L, Kruth J-P, Tan Y, Dewulf W (2015) Performance evaluation of CT measurements made on step gauges using statistical methodologies. CIRP - Journal of Manufacturing Science and Technology; 11:68-72.

[8] Arenhart FA, Nardelli VC, Donatelli GD (2015) Characterization of the metrological structural resolution of CT systems using a multi-wave standard. Proc. XXI IMEKO World Congress; Prague, Czech Republic.

[9] Arezki Y, Lepretre F, Psota P, Su R, Heikkinen V, Zhang X, et al. (2019) Material standards design for minimum zone fitting of freeform optics. Proc. euspen, Bilbao, Spain, June; pp. 264-267.

[10] ASME B89.4.1 (1997). Methods for Performance Evaluation of Coordinate Measuring Machines. American Society of Mechanical Engineers. New York. Addendums A (1998) and B (2001) then added. Superseded by ASME B89.4.10360.2 (2008).

[11] ASME B89.7.5 (2006). Technical Report – Guidelines for the Traceability of Dimensional Measurements. American Society of Mechanical Engineers. New York.

[12] Badami V, Liesener J, de Groot P (2019). Encoders graduating to extreme precision. Mikroniek 59/2:26-31.

[13] Baer G, Schindler J, Pruss C, Siepmann J, Osten W (2014) Fast and flexible non-null testing of aspheres and freeform surfaces with the tilted-wave-interferometer. Int. J. Optomechatron. 8:242–250.

[14] Balsamo A (2018) CCL/GD-06 CMCs of category "Standards of 1D point-to-point dimensions" – Guidelines. www.bipm.org/utils/common/pdf/CC/CCL/CCL-GD-6.pdf (accessed 2019-08-06).

[15] Balsamo A, Franke M, Trapet, Wäldele F, De Jonge L, Vanherck P (1997) Results of the CIRP-Euromet Intercomparison of Ball Plate-Based Techniques for Determining CMM Parametric Errors. CIRP Annals 46(1):463-466.

[16] Balsamo A, Frizza R, Picotto G, Corona D (2016) Design, manufacturing and calibration of a large ring segment. Proc. euspen, Nottingham, UK.

[17]Balsamo A, Zangirolami M (1998). Some practical aspects of long gauge block calibration. Proc. SPIE 3477:262-271.
[18]Bartl G, Becker P, Beckhoff B, Bettin H, Beyer E, Borys M, et al. (2017) A new ^{28}Si single crystal: counting the atoms for the new kilogram definition. Metrologia 54:693-715.
[19]Bartscher M, Busch K, Franke M, Schwenke H, Wäldele F (2000) New artifacts for calibration of large CMMs. ASPE Proceedings, 2000-10-22/27, Scottsdale (US-AZ).
[20]Bartscher M, Hilpert U, Goebbels J (2007) Enhancement and proof of accuracy of industrial computed tomography (CT) measurements. CIRP Annals, 56(1):495–8.
[21]Bartscher M, Illemann J. Neuschaefer-Rube U (2016) ISO Test Survey on Material Influence in Dimensional Computed Tomography. Case Studies in Nondestructive Testing and Evaluation, 6:79-92.
[22]Bartscher M, Neukamm M, Hilpert U, Neuschaefer-Rube U, Härtig F, Kniel K, et al. (2010) Achieving traceability of industrial computed tomography. Key Eng. 1:256–261.
[23]Bartscher M, Neukamm M, Koch M, Neuschaefer-Rube U, Staude A, Ehrig K, et al. (2010). Performance assessment of geometry measurements with micro-CT using a dismountable work-piece-near reference standard. Proc. of 10th European Conference on Non-Destructive testing, ECNDT 2010, Moscow, Russia.
[24]Bennett JM (1990) When is a Surface Clean? Optics & Photonics News 1:29-32.
[25]Bermudez C, Artigas R, Martinez P, Nolvi A, Jävinen M, Haeggström E, Kassamakov I (2018) Round Robin Test on V-shape Bio-imaging Transfer Standard for Determination of the Instrument Transfer Function of 3D Optical Profilers. Proc. SPIE 10499:1049923-1-9.
[26]Beutler A (2016) Metrology for the production process of aspheric lenses. Adv. Opt. Technol. 5:211–28.
[27]BIPM, CCL Length Services Classification (DimVIM), available in several languages from: www.bipm.org/en/committees/cc/ccl/dimvim.html (accessed 2019-08-06).
[28]BIPM, CCL, Report of 17th meeting (14-15 June 2018) to the CIPM; www.bipm.org/utils/common/pdf/CC/CCL/CCL17.pdf (accessed 2019-08-06).
[29]BIPM, Key Comparison Data Base, Calibration and Measurement Capabilities, Appendix C. https://kcdb.bipm.org/AppendixC/default.asp (accessed 2019-08-06).
[30]BIPM, Mise en Pratique of the Definition of the Metre. www.bipm.org/utils/en/pdf/si-mep/SI-App2-metre.pdf (accessed 2019-08-06).
[31]BIPM, SI Brochure 2019: The International System of Units (SI) (9th edition, 2019) www.bipm.org/en/publications/si-brochure/ (accessed 2019-08-06).
[32]Bitou Y, Seta K (2002). Wavelength scanning gauge block interferometer using a spatial light modulator. Jpn. J. Appl. Phys. 41, 384–8.
[33]Bodermann B, Buhr E, Li Z, Bosse H (2012). Quantitative Optical Microscopy at the Nanoscale: New Developments and Comparisons, in: Osten W and Reingand N (ed.) Optical Imaging and Metrology: Advanced Technologies, Wiley, Print ISBN:9783527410644.
[34]Boedecker S, Rembe C, Schmid H, Hageney T, Köhnlein T (2011) Calibration of the z-axis for large-scale scanning white-light interferometers. J Phys: Conf Series, 311:012027.
[35]Bolonin AA, Bolonin AA, Bolonina GA (2006). An interferometer for use with gauge blocks up to 1000 mm with laser and white-light sources. Meas. Tech. 49:845-849.
[36]Bosse H, Häßler-Grohne W (1997). New electron microscope system for pattern placement metrology. Proc. SPIE 3236; doi:10.1117/12.301186.
[37]Bosse H, Häßler-Grohne W, Flügge J, Köning R (2003). Final report on CCL-S3 supplementary line scale comparison Nano3. Metrologia 40, 04002.
[38]Bosse H, Kunzmann H, Pratt JR, et al. (2017). Contributions of precision engineering to the revision of the SI. CIRP Annals. 66 827–850.
[39]Bringmann B, Kung A (2005) A Measuring Artefact for True 3D Machine Testing and Calibration. CIRP Annals, 54(1):471–474.
[40]Buchta Z et al. (2012). Novel principle of contactless gauge block calibration. Sensors 12, 3350–8.
[41]Buice ES (2018) Alignment and Assembly Principles. In: Leach RK, Smith ST; Basics of Precision Engineering. CRC Press. New York.
[42]Byman V, Jaakkola T, Palosuo I, Lassila A (2018). High accuracy step gauge interferometer. Meas. Sci. Technol. 29, 054003.
[43]Byman V, Lassila A (2015). MIKES' primary phase stepping gauge block interferometer Meas. Sci. Technol. 26 084009.
[44]Carli L, Genta G, Cantatore A, Barbato G, De Chiffre L, Levi R (2011) Uncertainty evaluation for three-dimensional scanning electron microscope reconstructions based on the stereo-pair technique. Meas. Sci. Technol. 22(3):035103.
[45]Cantatore A, Andreasen JL, Carmignato S, Müller P, De Chiffre L (2011). Verification of a CT scanner using a miniature step gauge. Proc. euspen, 1:46-49.
[46]Carmignato S (2012) Accuracy of industrial computed tomography measurements: experimental results from an international comparison. CIRP Annals, 61-1:491-494.
[47]Carmignato S, De Chiffre L (2003) A new method for thread calibration on coordinate measuring machines. CIRP Annals, 52(1):447-450. doi: 10.1016/S0007-8506(07)60622-2.
[48]Carmignato S, Dewulf W, Leach R (2017) Industrial X-Ray Computed Tomography. Springer. doi: 10.1007/978-3-319-59573-3.
[49]Carmignato S, Dreossi D, Mancini L, Marinello F, Tromba G, Savio E (2009) Testing of X-ray microtomography system using a traceable geometrical standard. Meas. Sci. Technol. 20:084021, doi: 10.1088/0957-0233/20/8/084021.
[50]Carmignato S, Neuschaefer-Rube U, Schwenke H, Wendt K (2006) Tests and artefacts for determining the structural resolution of optical distance sensors for coordinate measurement. Proc. euspen, Baden, Austria, 1:62-65.
[51]Carmignato S, Savio E (2011) Traceable Volume Measurements Using Coordinate Measuring Systems. CIRP Annals, 60:519-522.
[52]Carmignato S, Voltan A, Savio E (2010) Metrological performance of optical coordinate measuring machines under industrial conditions. CIRP Annals, 59(1):497-500.
[53]Chao ZX, Tan SL, Xu G. (2009) Evaluation of the volumetric length measurement error of a micro-CMM using a mini sphere beam. Proc. LAMBDAMAP 2009, p.48–56.
[54]Chen X et al. (2017). Correlation and convolution filtering and image processing for pitch evaluation of 2D micro- and nano-scale gratings and lattices. Applied Optics 56-9, 2434-2443.
[55]Chen X et al. (2017). Self-calibration of Fizeau interferometer and planar scale gratings in Littrow setup. Optics Express 25-18, 21567-21582.
[56]Chen Y, Zhao X, Gao W, Hu G, Zhang S, Zhang D (2017) A Novel Multi-probe Method for Separating Spindle Radial Error from Artifact Roundness Error. Int. J. Adv. Manufac. Technol. 93:623-634.
[57]Chetwynd DG (2018) Materials Selection in Precision Mechanics. In: Leach RK, Smith ST; Basics of Precision Engineering. CRC Press. New York.
[58]Claverley JD, Leach RK (2013) Development of a three-dimensional vibrating tactile probe for miniature CMMs. Prec. Eng. 37:491-499.
[59]Claverley JD, Leach RK (2015). A review of the existing performance verification infrastructure for micro-CMMs. Prec. Eng. 39:1-15.
[60]Cresswell M, Guthrie W, Dixson R, Allen R A, Murabito C E, Martinez de Pinillos JV (2006). RM8111: Development of a Prototype Linewidth Standard. J. Res. Natl. Inst. Stand. Technol. 111:187–203.
[61]Dai G, Bütefisch S, Pohlenz F (2011) True 3D measurement on micro- and nano-structures. In: 56th international scientific colloquium. p. 12–6.
[62]Dai G et al. (2013). Reference nano-dimensional metrology by scanning transmission electron microscopy, Meas. Sci. Technol. 24/8, 085001:1-9.
[63]Dai G et al. (2014). Measurements of CD and sidewall profile of EUV photomask structures using CD-AFM and tilting-AFM, Meas. Sci. Technol., 25-4.
[64]Dai G et al. (2017). Comparison of line width calibration using critical dimension atomic force microscopes between PTB and NIST. Meas. Sci. Technol. 28/6:065010.
[65]Dai G, Seeger B, Weimann T, Xie W, Hüser D, Tutsch R (2019) Development of a novel material measure for characterising instrument transfer function (ITF) considering angular-dependent asymmetries of areal surface topography measuring instruments. Proc. euspen, Bilbao, Spain, Jun.
[66]Dai G, Wolff H, Pohlenz F, Bütefisch S, Danzebrink H-U (2010) Normale und Kalibrierverfahren für Mikro- und Nano-Koordinatenmessgeräte. VDI-Berichte 2120:95-111.
[67]De Chiffre L, Carli L, Eriksen RS (2011) Multiple height calibration artefact for 3D microscopy. CIRP Annals 60(1):535-538.
[68]De Chiffre L, Carmignato S, Kruth J-P, Schmitt R, Weckenmann A (2014). Industrial applications of computed tomography. CIRP Annals, 63(2):655-677.
[69]De Chiffre L, González-Madruga D, et al. (2018) Accurate measurements in a production environment using dynamic length metrology (DLM). Procedia CIRP, 75:343–348.
[70]De Chiffre L, Kunzmann H, Peggs G, Lucca DA, 2003, Surfaces in Precision Engineering, Micro-engineering and Nano-technology. CIRP Annals, 52/2, 561-577.
[71]De Chiffre L, Hansen HN, Morace RE (2006). Metrological validation of an optomechanical hole plate for the verification of optical and multiprobing coordinate measuring machines. Proc. euspen, Baden, Austria.
[72]De Chiffre L, Carmignato S, Cantatore A, Jensen JD (2009). Replica calibration artefacts for optical 3D scanning of micro parts. Proc. euspen; 352–355.
[73]Decker JE et al. (2011). Evaluation of uncertainty in grating pitch measurement by optical diffraction using Monte Carlo methods. Meas. Sci. Technol. 22, 027001.
[74]Decker JE, Schödel R, Bönsch G (2004). Considerations for the evaluation of measurement uncertainty in interferometric gauge block calibration applying methods of phase step interferometry. Metrologia, 41:L11–L17.
[75]de Groot P, Colonna de Lega X, Sykora DM, Deck L (2012) The meaning and measure of lateral resolution for surface profiling interferometers. Optics and Photonics News. 23:10-13.
[76]Dewulf W, Ferrucci M, Ametova E, et al. (2018) Enhanced dimensional measurement by fast determination and compensation of geometrical misalignments of X-ray computed tomography instruments. CIRP Annals 67(1):523-526.
[77]Dixson RG, Allen RA, Guthrie WF, Cresswell MW (2005). Traceable calibration of critical-dimension atomic force microscope linewidth measurements with nanometer uncertainty. J. Vac. Sci. Technol. B 23/6:3028–3032.
[78]Doiron T et al. (2005). The Gage Block Handbook. NIST Monogr. 180.
[79]Doiron T (2007). 20 degrees C - A short history of the standard reference temperature for industrial dimensional measurements. J. Res. Natl. Inst. Stand. Technol. 112, 1-23.
[80]Dury M, Woodward S, Brown S. McCarthy MB (2016) Characterising 3D Optical Scanner Measurement Performance for Precision Engineering. Proc ASPE 167-172.
[81]Ehrig W, Neuschaefer-Rube U (2007) Artefacts with rough surfaces for verification of optical microsensors. Proc. SPIE, 6616-1:661626.
[82]Ehrig W, Neuschaefer-Rube U, Neugebauer M, Meeß R (2009) Traceable optical coordinate metrology applications for the micro range. Proc SPIE 7239:72390G.
[83]Eifler M, Schneider F, Seewig J, Kirsch B, Aurich JC (2016) Manufacturing of new roughness standards for the linearity of the vertical axis–Feasibility study and optimization. Engineering Science and Technology. 19:1993-2001.
[84]Eifler M, Hering J, Freymann GV, Seewig J. (2018) Calibration sample for arbitrary metrological characteristics of optical topography measuring instruments. Opt. Express 26:16609-16623.
[85]Estler T (1985). High-accuracy displacement interferometry in air. Applied Optics, 24 6 808-815.
[86]Estler T, Edmundson KL, Peggs GN, Parker DH (2002) Large-scale metrology - an update. CIRP Annals, 51(2):587–60.
[87]EURAMET CG-2 (2011). Calibration of Gauge Block Comparators. EURAMET e.V., Technical Committee for Length. Braunschweig. (link).
[88]EURAMET CG-6 (2011). Extent of Calibration for Cylindrical Diameter Standards. EURAMET e.V., Technical Committee for Length. Braunschweig. (link).

[89]EURAMET CG-23 (2018). Guidelines on the Calibration of Angular Encoders. EURAMET e.V., Technical Committee for Length. Braunschweig. (link)
[90]EURAMET.L-K5.2016 (2016). Calibration of 1-D CMM artefacts: Step Gauges (EURAMET project 1365). Technical protocol. National Physical Laboratory, Teddington, UK. https://kcdb.bipm.org/appendixB/appbresults/EURAMET.L-K5.2016/EURAMET.L-K5-2016_TP.pdf (accessed 2019-08-06).
[91]Evans CL, Hocken RJ, Estler TW (1996) Self-Calibration: Reversal, Redundancy, Error Separation, and 'Absolute Testing'. CIRP Annals, 45(2):617-634.
[92]Fang FZ, Zhang XD, Weckenmann A, Zhang GX, Evans C (2013) Manufacturing and measurement of freeform optics. CIRP Annals, 62:823-846.
[93]Ferrucci M, Haitjema H, Leach RK (2018) Dimensional Metrology. In: Leach RK, Smith ST; Basics of Precision Engineering. CRC Press. New York.
[94]Flügge J et al. (2010). Long term stability of Suprasil line scales and gauge blocks. Proc. euspen, vol. 1, paper 3.35.
[95]Franceschini F, Galetto M, Maisano DA, Mastrogiacomo L, Pralio B (2011) Distributed Large-Scale Dimensional Metrology: New Insights. Springer, London.
[96]Galantucci LM, Pesce M, Lavecchia F (2015) A stereo photogrammetry scanning methodology, for precise and accurate 3D digitization of small parts with sub-millimeter sized features. CIRP Annals, 64(1):507–510.
[97]Galetto M, Mastrogiacomo L, Maisano D, Franceschini F (2016) Uncertainty evaluation of distributed Large-Scale-Metrology systems by a Monte Carlo approach. CIRP Annals, 65(1):491-494.
[98]Galetto M, Mastrogiacomo L, Moroni G, Petrò S (2015) Artifact-based calibration and performance verification of the MScMS-II. Procedia CIRP, 27:77-83.
[99]Galetto M, Mastrogiacomo L, Pralio B (2011) MScMS-II: An innovative IR-based indoor coordinate measuring system for large-scale metrology applications. International Journal of Advanced Manufacturing Technology, 52(1-4):291-302.
[100] Garnaes J, Dirscherl K (2008). NANO5 – 2D Grating – Final report. Metrologia 45, 04003.
[101] Garnaes J et al. (2008). The role of 2D gratings for accurate dissemination of the nanometre. Proc. Nanoscale 2008. Turin (IT).
[102] Gameros A, De Chiffre L, Siller HR, Hiller J, Genta G (2015) A reverse engineering methodology for nickel alloy turbine blades with internal features. CIRP - Journal of Manufacturing Science and Technology, 9:116-124.
[103] Gans F, Liebe R, Richter J, Schätz Th, Hauffe B, Hillmann F, et al. (2005). Results of a round robin measurement on a new CD mask standard. 21th European Mask and Lithography Conference EMLC; GMM-Fachbericht: 45:109-119.
[104] Gao W, Haitjema H, Fang F Z, Leach RK, Cheung CF, Savio E, Linares JM (2019). On-machine and in-process surface metrology for precision manufacturing. CIRP Annals, 68(2):843-866.
[105] Gao W, Kim SW, et al. (2015). Measurement technologies for precision positioning. CIRP Annals, 64(2):773–796.
[106] Gao W, Kimura A (2007). A Three-axis Displacement Sensor with Nanometric Resolution. CIRP Annals, 56(1):529-532.
[107] Gao W, Kimura A (2010). A fast evaluation method for pitch deviation and out-of-flatness of a planar scale grating. CIRP Annals, 59(1):505-508.
[108] Gaoliang D et al. (2005). Accurate and traceable calibration of one-dimensional gratings. Meas. Sci. Technol. 16, 1241.
[109] Gaoliang D et al. (2007). Accurate and traceable calibration of two-dimensional gratings Meas. Sci. Technol. 18, 415.
[110] Geckeler RD (2006) Shearing deflectometry as a flatness standard: Comparison with a mercury mirror and absolute interferometry. Proc. euspen, Baden, Austria 394-397.
[111] Geckeler RD, et al. (2015). New frontiers in angle metrology at the PTB. Measurement 73:231–238.
[112] Geckeler RD et al. (2018) Angle comparison using an autocollimator. Metrologia,55 04001 1–57, Technical Supplement.
[113] Geckeler RD et al. (2018) Influence of the air's refractive index on precision angle metrology with autocollimators. Meas. Sci. Technol. 29:1–9.
[114] Ghandali P, Khameneifar F, Mayer JRR (2019) A pseudo-3D ball lattice artifact and method for evaluating the metrological performance of structured-light 3D scanners. Optics and Lasers in Engineering, 121:87-95.
[115] Giusca CL, Leach RK, Helery F, Gutauskas T, Nimishakavi L (2012) Calibration of the Scales of Areal Surface Topography Measuring Instruments: Part 1 - Measurement Noise and Residual Flatness. Meas. Sci. Technol. 23:035008.
[116] Goch G (2003) Gear Metrology. CIRP Annals, 52(2):659-695.
[117] Guerra MG, Volpone C, Galantucci LM, Percoco G (2018) Photogrammetric Measurements of 3D Printed Microfluidic Devices. Additive Manufacturing, 21:53–62.
[118] Gupta M, Agrawal A, Veeraraghavan A, Narasimhan SG (2013) A Practical Approach to 3D Scanning in the Presence of Interreflections, Subsurface Scattering and Defocus. Int. J. Computer Vision 102:33-55.
[119] Häfner B, Lanza G (2017) Function-oriented measurements and uncertainty evaluation of micro-gears for lifetime prognosis. CIRP Annals, 66(1):475-478.
[120] Hansen HN, Carneiro K, Haitjema H, De Chiffre L (2006) Dimensional Micro and Nano Metrology. CIRP Annals, 52(2):721-744.
[121] Hansen HN, De Chiffre L (1997) A combined optical and mechanical reference artefact for coordinate measuring machines. CIRP Annals, 46(1):467-470.
[122] Haitjema H (2011) Roundness Measuring Device Calibration Tool, and Calibration Method for the Roundness Measuring Device. Japanese Patent JP4690276(B2).
[123] Haitjema H (2015) Revisiting the Multi-step Method: Enhanced Error Separation and Reduced Amount of Measurements. CIRP Annals, 64:491-494.
[124] Haitjema H (2016) Flatness. In: Laperrière L, Reinhart G, Tolio T, Chatti S, CIRP Encyclopaedia of Production Engineering. Springer-Verlag: Berlin. 2nd edition.
[125] Haitjema H et al. (1998). Long gauge block measurements based on a Twyman-Green interferometer and three stabilized lasers. Proc. SPIE 3477, 25–34.
[126] Haitjema H, Pril WO, Schellekens PHJ (2001) Development of a Silicon-Based Nanoprobe System for 3-D Measurements. CIRP Annals, 50(1):365-368.
[127] Harding K (2013) Handbook of Optical Dimensional Metrology. CRC Press. New York.
[128] Häßler-Grohne W et al. (2011) Current limitations of SEM and AFM metrology for the characterization of 3D nanostructures, Meas. Sci. Technol., 22-9.
[129] Häusler G, Faber C, Olesch E, Ettl S (2013) Deflectometry versus interferometry. Proc. SPIE 8788:87881C.
[130] Hermanek P, Carmignato S (2016) Reference object for evaluating the accuracy of porosity measurements by X-ray computed tomography. Case Studies in Nondestructive Testing and Evaluation. 6:122-127.
[131] Hermanek P, Carmignato S (2017). Porosity measurements by X-ray computed tomography: Accuracy evaluation using a calibrated object. Prec. Eng., 49:377-387.
[132] Hermanek, P., Zanini, F., Carmignato, S. (2019). Traceable Porosity Measurements in Industrial Components Using X-Ray Computed Tomography. Journal of Manufacturing Science and Engineering, Transactions of the ASME. 141(5):051004.
[133] Hidaka K (2006) Study of a small-sized Ultrasonic Probe. CIRP Annals, 55(1):567-570.
[134] Hilger A (1939). Gauge comparing and absolute length measuring interferometers. J. Sci. Instrum. 16, 163.
[135] Hocken RJ, Pereira PH (2011) Coordinate Measuring Machines and Systems. 2nd ed. CRC Press. New York.
[136] Ikonen E et al. (1993). Gauge-block Interferometer Based on One Stabilized Laser and a White-light Source. Metrologia 30-95.
[137] ILAC – International Laboratory Accreditation Cooperation. National Accreditation bodies listed at https://ilac.org/signatory-search (accessed 2019-08-06) maintain national databases of accredited laboratories.
[138] Illemann J, Bartscher M, Jusko O, Härtig F, Neuschaefer-Rube U, Wendt K (2014) Procedure and reference standard to determine the structural resolution in coordinate metrology. Meas. Sci. Technol. 25 064015.
[139] Imkamp D, Berthold J, Heizmann M, Kniel K, Manske E, Peterek M, Schmitt R, Seidler J, Sommer K-D (2016). Challenges and trends in manufacturing measurement technology - the "Industrie 4.0" concept. J. Sens. Sens. Syst., 5:325-335.
[140] ISO 1 (2016). Geometrical product specifications (GPS) – Standard reference temperature for the specification of geometrical and dimensional properties. International Organization for Standardization. Geneva.
[141] ISO 230-1 (2012). Test code for machine tools – Part 1: Geometric accuracy of machines operating under no-load or quasi-static conditions. International Organization for Standardization. Geneva.
[142] ISO/TR 230-11 (2018). Test code for machine tools – Part 11: Measuring instruments suitable for machine tool geometry tests. International Organization for Standardization. Geneva.
[143] ISO 1101 (2017). Geometrical Product Specifications (GPS) – Geometrical Tolerancing – Tolerances of Form, Orientation, Location and Run-out. International Organization for Standardization. Geneva.
[144] ISO 3650 (1998). Geometrical Product Specifications (GPS) – Length standards – Gauge blocks. International Organization for Standardization. Geneva.
[145] ISO 5436-1 (2000). Geometrical Product Specification (GPS) – Surface Texture: Profile Method – Measurement Standards – Material Measures. International Organization for Standardization, Geneva.
[146] ISO 8015 (2011). Geometrical product specifications (GPS) – Fundamentals – Concepts, principles and rules. International Organization for Standardization. Geneva.
[147] ISO 10360-2 (2009). Geometrical product specifications (GPS) – Acceptance and reverification tests for coordinate measuring machines (CMM) – Part 2: CMMs used for measuring linear dimensions. International Organization for Standardization. Geneva.
[148] ISO 10360-7 (2011). Geometrical product specifications (GPS) – Acceptance and reverification tests for coordinate measuring machines (CMM) – Part 7: CMMs equipped with imaging probing systems. International Organization for Standardization. Geneva.
[149] ISO 10791-7 (2020). Test conditions for machining centres – Part 7: Accuracy of finished test pieces. International Organization for Standardization. Geneva.
[150] ISO 12780-1 (2011). Geometrical Product Specifications (GPS) – Straightness Part 1: Vocabulary and Parameters of Straightness. International Organization for Standardization. Geneva.
[151] ISO 12781-1 (2011). Geometrical Product Specifications (GPS) – Flatness Part 1: Vocabulary and Parameters of Flatness. International Organization for Standardization. Geneva.
[152] ISO 15530-3 (2011). Geometrical product specifications (GPS) – Coordinate measuring machines (CMM): Technique for determining the uncertainty of measurement – Part 3: Use of calibrated workpieces or measurement standards. International Organization for Standardization, Geneva.
[153] ISO/TR 16015 (2003). Geometrical product specifications (GPS) – Systematic errors and contributions to measurement uncertainty of length measurement due to thermal influences. International Organization for Standardization. Geneva.
[154] ISO 17450-1 (2011). Geometrical product specifications (GPS) – General concepts – Part 1: Model for geometrical specification and verification. International Organization for Standardization. Geneva.
[155] ISO 17450-2 (2012). Geometrical product specifications (GPS) – General concepts – Part 2: Basic tenets, specifications, operators, uncertainties and ambiguities. International Organization for Standardization. Geneva.
[156] ISO/IEC 17025 (2017). General requirements for the competence of testing and calibration laboratories. International Organization for Standardization. Geneva.

[157] ISO 25178-70 (2014). Geometrical Product Specification (GPS) – Surface Texture: Areal – Part 70: Material Measures. International Organization for Standardization, Geneva.
[158] ISO 25178-600 (2019). Geometrical Product Specification (GPS) – Surface Texture: Areal – Part 600: Metrological characteristics for areal topography measuring methods. International Organization for Standardization, Geneva.
[159] ISO/ASTM 52902 (2019). Additive manufacturing – Test artifacts – Geometric capability assessment of additive manufacturing systems. International Organization for Standardization. Geneva.
[160] Jansson A, Hermanek P, Pejryd L, Carmignato S (2018) Multi-material gap measurements using dual-energy computed tomography. Prec. Eng., 54:420-426.
[161] Jin J et al. (2006). Absolute length calibration of gauge blocks using optical comb of a femtosecond pulse laser. Opt. Express 14, 5968–74.
[162] JCGM 100 (2008). Evaluation of measurement data – Guide to the expression of uncertainty in measurement. Joint Committee for Guides in Metrology. Paris.
[163] JCGM 200 (2012). International vocabulary of metrology – Basic and general concepts and associated terms (VIM), 3rd ed., 2008 version with minor corrections.
[164] Johannson CE (1901). Gauge Block Sets for Precision Measurement. SE patent No. 17017.
[165] JRP Crystal, Crystalline and self-assembled structures as length standards, Joint Research Project, www.ptb.de/emrp/sib61-home.html (accessed 2019-08-06).
[166] Jusko O, Lüdicke F (1999) Novel multi-wave standards for the calibration of form measuring instruments. Proc. euspen, 2:299-302.
[167] Jusko O et al. (2006). CCL-K5: CMM 1D: Step gauge and ball bars: Final report. Metrologia 43, 04006.
[168] Just A, et al. (2009) Comparison of angle standards with the aid of a high-resolution angle encoder. Prec. Eng. 33(4):530-533.
[169] Keferstein C P, Marxer M, Götti R, Thalmann R, Jordi T, Andräs M, Becker J (2012) Universal High Precision Reference Spheres for Multisensor Coordinate Measuring Machines. CIRP Annals, 61:487–490.
[170] Keksel A, Eifler M, Seewig J (2018) Modeling of topography measuring instruments transfer functions by time series models. Meas. Sci. Technol. 29:095012.
[171] Kim JA et al. (2010). An interferometric Abbe-type comparator for the calibration of internal and external diameter standards. Meas. Sci. Technol. 21 075109.
[172] Kimura A et al. (2007). Design and Construction of a Surface Encoder with Dual Sine-Grids. Int. J. of Prec. Eng. And Manuf. 8-2, 20-25.
[173] Köning R, Bodermann B, Bergmann D, Buhr E, Häßler-Grohne W, Flügge J, Bosse H (2011) Towards traceable bidirectional optical size measurements for optical coordinate measuring machine metrology. Proc. MacroScale, Bern-Wabern.
[174] Kruger OA (2007) Final report on CCL-K3: Calibration of angle standards. Metrologia, 46, Technical Supplement.
[175] Kruger O, Walt F, Greeff P (2011) Ball and hole plate development for evaluation of µCMM. Proc. MacroScale; October; p. 1–5.
[176] Kruth J-P, Bartscher M, Carmignato S, Schmitt R, De Chiffre L, Weckenmann A (2011) Computed tomography for dimensional metrology. CIRP Annals, 60:821–42.
[177] Küng A, Meli F. (2007) Comparison of three independent calibration methods applied to an ultra-precision micro-CMM. Proc. euspen, Cranfield, UK; 1:230–233.
[178] Kunzmann H, Pfeifer T, Flügge J (1993). Scales vs Laser Interferometers - Performance and Comparison of Two Measuring Systems. CIRP Annals, 42-2:753-767.
[179] Kunzmann, H., Pfeifer, T., Schmitt, R., Schwenke, H., Weckenmann, A., 2005, Productive Metrology - Adding Value to Manufacture, CIRP Annals, 54/2,155-168.
[180] Kuriyama Y et al. (2006). Development of a New Interferometric Measurement System for Determining the Main Characteristics of Gauge Blocks. CIRP Annals, 55, 563–6.
[181] Lanza G, Viering B (2011) A novel standard for the experimental estimation of the uncertainty of measurement for micro gear measurements. CIRP Annals, 60(1):543-546.
[182] Lassila A et al. (2015). Wave front and phase correction for double-ended gauge block interferometry. Metrologia 52, 708.
[183] Lavecchia F, Guerra MG, Galantucci LM (2018). Performance verification of a photogrammetric scanning system for micro-parts using a three-dimensional artefact: adjustment and calibration. Int J Adv Manuf Technol, 96/9–12: 4267–4279.
[184] Leach RK (1998) Measurement of a Correction for the Phase Change on Reflection due to Surface Roughness. Proc. SPIE 3477:138-152.
[185] Leach RK (2011) Optical Measurement of Surface Topography. Springer. Berlin.
[186] Leach RK (2014) Fundamental Principles of Engineering Nanometrology. Elsevier. Amsterdam.
[187] Leach RK, Bourell D, Carmignato S, Donmez A, Senin N, Dewulf W (2019). Geometrical metrology for metal additive manufacturing. CIRP Annals, 68-2:677-700.
[188] Leach RK, de Groot P, Haitjema H (2018) Infidelity and the calibration of surface topography measuring instruments. Proc. ASPE, Las Vegas, USA, Nov.
[189] Leach RK, Giusca CL, Rickens K, Riemer O, Rubert P (2014) Development of a low-cost artefact for performance verifying surface topography measuring instruments. Surf. Topog.: Met. Prop. 2:025002.
[190] Leach RK, Giusca CL, Haitjema H, Evans CJ, Jiang X (2015) Calibration and Verification of Areal Surface Texture Measuring Instruments. CIRP Annals, 64:797-813.
[191] Leach RK. Smith ST (2018) Basics of Precision Engineering. CRC Press. New York.
[192] Lee, J., Bagheri, B., Kao, H.-A., 2015, A Cyber-Physical Systems architecture for Industry 4.0-based manufacturing systems, Manuf. Letters, 3, 18-23.
[193] Lei LH et al. (2011). Fast and Accurate Calibration of 1D and 2D Gratings, Advanced Materials Research 317-319, 2196-2203.
[194] Lewis AJ (1993). Absolute length measurement using multiple-wavelength phase-stepping interferometry. PhD dissertation, Imperial College, London.
[195] Lewis AJ et al. (2010). Long-term study of gauge block interferometer performance and gauge block stability. Metrologia 47, 473–86.
[196] Li T, Birch KG (1987) A practical determination of the phase change at reflection. IEEE Trans. Instrum. Meas. IM-36:547–50.
[197] Li X et al. (2013). A six-degree-of-freedom surface encoder for precision positioning of a planar motion stage. Prec. Eng. 37:771–781.
[198] Linkeová I, Skalník P, Zelený V (2015) Calibrated CAD model of freeform standard. Proc. XXI IMEKO World Congress, TC14-301, Prague, Czech Republic.
[199] Lyngby RA, Nielsen E, De Chiffre L, Aanæs H, Dahl AB (2019) Development and metrological validation of a new automated scanner system for freeform measurements on wind turbine blades in the production. Prec. Eng. 56:255-266.
[200] Malinovsky I et al. (1999). Toward subnanometer uncertainty in interferometric length measurements of short gauge blocks. Appl. Opt. 38, 101–12.
[201] Madsen MH et al. (2016). Alignment-free characterization of 2D gratings. Applied Optics 55-2, 317-322.
[202] Marinello F, Savio E, Carmignato S, De Chiffre L (2008) Calibration artefact for the microscale with high aspect ratio: the fiber gauge. CIRP Annals, 57(1);497-500; doi: 10.1016/j.cirp.2008.03.086.
[203] Marsh E (2010) Precision Spindle Metrology. DEStech Publications.
[204] Marposs, www.marposs.com/eng/family/calibration-masters (accessed 2019-08-06).
[205] Matsumoto H et al. (2008). Remote Measurements of Practical Length Standards Using Optical Fiber Networks and Low-Coherence Interferometers. Jpn. J. Appl. Phys. 47, 8590–4.
[206] Matsuzaki K, Sato O, Fujimoto H, Abe M, Takatsuji T (2017) Feasibility of Dimensional Gauges Made of Plastic Used for Acceptance Tests of Coordinate Measuring Systems. Prec. Eng. 50:308-312.
[207] Mayer JRR, Hashemiboroujeni H (2017) A ball dome artefact for coordinate metrology performance evaluation of a five axis machine tool. CIRP Annals, 66(1):479–482.
[208] McCarthy MB, Brown SB, Evenden A, Robinson AD (2011). NPL freeform artifact for verification of non-contact measuring systems Proc. SPIE 7864 78640K.
[209] Mohr PJ et al. (2018). Data and analysis for the CODATA 2017 special fundamental constants adjustment for the revision of the SI. Metrologia, 55:125-146.
[210] Monostori L, Kádár B, Bauernhansl T, et al. (2016) Cyber-physical systems in manufacturing. CIRP Annals, 65(2):621-641.
[211] Moore WR (1999) Foundations of Mechanical Accuracy. Moore Special Tool Co.
[212] Mutilba U, Gomez-Acedo E, Kortaberria G, Olarra A, Yagüe-Fabra JA (2017) Traceability of On-Machine Tool Measurement: A Review. Sensors, 17(7):1605.
[213] Naqvi SSH, Krukar RH, et al. (1994). Etch depth estimation of large-period silicon gratings with multivariate calibration of rigorously simulated diffraction profiles. J. Opt. Soc. Am. A 11, 2485-2493.
[214] Neugebauer M (2011) EURAMET Project 1105 – Bilateral comparison on micro-CMM artefacts between PTB and METAS – final report. Braunschweig, DE.
[215] Neugebauer M, Härtig, F, Jusko O, Neuschaefer-Rube U (2008). Recent developments in micro CMM measurement technique at PTB. In: Proc. ACMC workshop.
[216] Neugebauer M, Neuschaefer-Rube U (2005) A new micro artefact for testing of optical and tactile sensors. Proc. euspen, vol.1, p. 201–204.
[217] Neuschaefer-Rube U, Neugebauer M, Dziomba T, Danzebrink H-U, Koenders L, Bosse H (2014) New developments of measurement standards and procedures for micro and nanometrology at the PTB. 11th IMEKO TC14 Sympos. on Laser Metrology for Precision Measurement and Inspection in Industry, LMPMI 2014, pp. 13-18.
[218] Neuschaefer-Rube, U., Neugebauer, M., Ehrig, W., Bartscher, M., Hilpert, U. (2008). Tactile and optical microsensors: Test procedures and standards. Meas. Sci. Technol. 19/8:084010.
[219] Nicolaus RA, Bartl G (2016) Spherical interferometry for the characterization of precision spheres. Surf. Topogr.: Metrol. Prop. 4:034007.
[220] Nicolaus RA, Bartl G, Peter A, Kuhn E, Mai T (2017) Volume determination of two spheres of a new ^{28}Si crystal at PTB. Metrologia. 54:512-515.
[221] Nijsse G J P (2001) Linear Motion Systems. A Modular Approach for Improved Straightness Performance. PhD Thesis: TU Delft.
[222] Nimishankavi LP, Jones C, O'Connor D, Giusca CL (2019) NPL Areal Standard: a multi-function calibration artefact for surface topography measuring instruments. Proc. Lamdamap, Sheffield, UK 69-72.
[223] Noste T, Hopper L, Miller J, Evans C (2019) Task specific uncertainty in measurement of freeform optics. Proc. euspen, Bilbao, Spain, Jun.
[224] Osawa S at al. (2006). Development of an Interferometric Coordinate Measuring Machine Used for Step-gauge Calibration. J. Jpn Soc. for Prec. Eng. 68-5, 687-691.
[225] Palousek D, Omasta M, Koutny D, Bednar J, Koutecky T, Dokoupil F (2015) Effect of Matte Coating on 3D Optical Measurement Accuracy. Optical Materials 40:1-9.
[226] Parks RE (2018). Alignment with axicon plane gratings. Proc. SPIE 10747.
[227] Parks RE, Ziegert JC, Groover J (2017). Computer Generated Holograms as 3-Dimensional Calibration Artifacts. ASPE Proceedings, 67:117-120.
[228] Paviotti A, et al. (2009) Estimating angle-dependent systematic error and measurement uncertainty for a conoscopic holography measurement system. Proc. SPIE 7239:72390Z.
[229] Percoco G, Guerra MG, Sanchez Salmeron AJ, Galantucci LM (2017). Experimental Investigation on camera calibration for 3D photogrammetric scanning of micro-features for micrometric resolution. Int J Adv Manuf Technol, 91/9-12:2935-2947.
[230] Pérez-Pacheco E, Cauich-Cupul JI, Valadez-González A, Herrera-Franco PJ (2013) Effect of moisture absorption on the mechanical behaviour of carbon fiber/epoxy matrix composites. Journal of Material Science 48:1873–1882.

[231] Picotto GB et al. (2011). The INRIM 1D comparator with a new interferometric set-up for measurement of diameter gauges and linear artefacts. Proc. of Macroscale, Wabern (CH), 2011-10-04/06, doi:10.7795/810.20130620o.
[232] Pinard L, Michel C, Sassolas B, Balzarini L, Degallaix J, Dolique V, Flaminio R, Forest D, Granata M, Lagrange B, Straniero N (2017) Mirrors Used in the LIGO Interferometers for First Detection of Gravitational Waves. Appl. Opt. 56:C11-C115.
[233] Phillips SD, Borchardt B, Doiron T, Henry† J (1993). Properties of free-standing ball bar systems. Prec. Eng. 15-1, 16-24.
[234] Phillips SD et al. (2016). The 2016 Revision of ISO 1 – Standard Reference Temperature for the Specification of Geometrical and Dimensional Properties. J. Res. Natl. Inst. Stand. Technol. 121, 498-504.
[235] Powell I, Goulet E (1998) Absolute Figure Measurements with a Liquid-flat Reference. Appl. Opt. 37:2579-2588.
[236] Probst R, Wittekopf R, Krause M, Dangschat H, Ernst A (1998) The new PTB angle comparator, Meas. Sci. Technol. 9:1059–1066.
[237] Qian S et al. (2015) Approaching sub-50 nanoradian measurements by reducing the saw-tooth deviation of the autocollimator in the Nano-Optic-Measuring Machine. Nuclear Instruments and Methods in Physics Research A, 785:206–212.
[238] Quabis S, Schulz M, Ehret G, Asar M, Balling P, Křen P, Bergmans RH, Küng A, Lassila A, Putland D, Williams D, Pirée H, Priet E, Pérez M, Svedova L, Ramotowski Z, Vannoni M, Hungwe F, Kang Y (2017) Intercomparison of Flatness Measurements of an Optical Flat at Apertures of up to 150 mm in Diameter. Metrologia 54:85-93.
[239] Raab M et al. (2018). Using DNA origami nanorulers as traceable distance measurement standards and nanoscopic benchmark structures. Sci. Rep., 8:1780.
[240] Reiter M, de Oliveira FB, Bartscher M, Gusenbauer C, Kastner J (2019) Case Study of Empirical Beam Hardening Correction Methods for Dimensional X-ray Computed Tomography Using a Dedicated Multi-material Reference Standard. Journal of Nondestructive Evaluation, 38(1),10.
[241] Renishaw, www.renishaw.com/en/equator-gauging-explained--13465 (accessed 2019-08-06).
[242] Riehle R (1998). Use of optical frequency standards for measurements of dimensional stability. Meas. Sci. Technol. 9, 1042.
[243] Ritter M, Dziomba T, Kranzmann A, Koenders L (2007) A landmark-based 3D calibration strategy for SPM. Meas. Sci. Technol. 18:404-414.
[244] Rivas Santos V M, Thompson A, Sims-Waterhouse D, Maskery I, Woolliams P, Leach R K (2020) Design and characterisation of an additive manufacturing benchmarking artefact following a design-for-metrology approach. Additive Manufacturing, 32:100964.
[245] Roger G, Flack D McCarthy M (2007) A review of industrial capabilities to measure freeform surfaces. NPL report, DEPC-EM 014, National Physical Laboratory, Teddington, UK.
[246] Rothemund PW (2006). Folding DNA to create nanoscale shapes and patterns. Nature 440:297–302.
[247] Sammartini MP, De Chiffre L (2000) Development and validation of a new reference cylindrical gear for pitch measurement. Prec. Eng. 24/4:302-309.
[248] Santolaria J, Aguilar JJ, Yagüe JA, Pastor J (2008) Kinematic parameter estimation technique for calibration and repeatability improvement of articulated arm coordinate measuring machines. Prec. Eng. 32/4:251-268.
[249] Sato O, Osawa S, Takatsuji T, Murakami M, Haradaz R (2008) Test artefacts for the verification of optical digitizers. Key Engineering Materials, 381-382:553-556.
[250] Savio E (2012). A methodology for the quantification of value-adding by manufacturing metrology, CIRP Annals, 61/1, 503-506.
[251] Savio E, De Chiffre L (2002) An artefact for traceable freeform measurements on coordinate measuring machines. Prec. Eng. 26:58-68.
[252] Savio E, De Chiffre L, Carmignato S, Meinertz J (2016) Economic benefits of metrology in manufacturing, CIRP Annals, 65(1): 495-498.
[253] Savio, E, De Chiffre L, Schmitt R (2007) Metrology of freeform shaped parts, CIRP Annals, 53(2):810-835.
[254] Savio E, Hansen HN, De Chiffre L (2002) Approaches to the Calibration of Freeform Artefacts on Coordinate Measuring Machines. CIRP Annals, 51(1):433-436.
[255] Sawabe M et al. (2004). A New Vacuum Interferometric Comparator for Calibrating the Fine Linear Encoders and Scales. Prec. Eng. 28:320–328.
[256] Schachtschneider R, Fortmeier I, Stavridis M, Asfour J, Berger G, Bergmann RB, et al. (2018) Interlaboratory comparison measurements of aspheres. Meas. Sci. Technol. 29:055010.
[257] Schalck R (2013) The Proper Care of Optics: Cleaning, Handling, Storage, and Shipping. SPIE Press.
[258] Schmitt RH, Peterek M, Morse E, Knapp W, Galetto M, Härtig F, Goch G, Hughes B, Forbes A, Estler WT (2016). Advances in Large-Scale Metrology – Review and future trends. CIRP Annals, 65/2:643-666.
[259] Schödel R (2008). Ultra high accuracy thermal expansion measurements with PTB's precision interferometer. Meas. Sci. Technol. 19, 8, 084003:1-11.
[260] Schödel R (2009). High accuracy measurements of long-term stability of material with PTB's Precision Interferometer. Proc. of SPIE 7133, 2, 71333J:1-9.
[261] Schumann M et al. (2019) The spatial angle autocollimator calibrator: optimised model, uncertainty budget and experimental validation. Metrologia 56 015011.
[262] Schwenke H, Knapp W, Haitjema H, Weckenmann A, Schmitt R, Delbressine F (2008) Geometric Error Measurement and Compensation of Machines - An Update. CIRP Annals, 57:660-675.
[263] Schwenke H, Wäldele F, Wendt K (1998) Abnahme, Überwachung und Kalibrierung von flexiblen industriemeßsystemen mit CCD-Kameras, PTB, Braunschweig, Germany.
[264] Seewig J, Eifler M, Wiora G (2014) Unambiguous evaluation of a chirp measurement standard. Surf. Topog. Metr. Prop. 2:045003.
[265] Shilling M, Tran HD, Claudet AA, Oliver A, Bauer T (2010) Silicon Bulk Micromachined Hybrid Dimensional Artifact. Sandia Report SAND2010-1371, Sandia National Laboratories, Albuquerque, New Mexico, USA.
[266] Smith GT (2016) Artefacts for Machine Verification. In: Machine Tool Metrology. Springer, Cham; doi: 10.1007/978-3-319-25109-7_5.
[267] Smith S, Tsiamis A, et al. (2009). Comparison of Measurement Techniques for Linewidth Metrology on Advanced Photomasks. IEEE Trans. on semiconductor manufacturing, vol. 22(1):72-79.
[268] SMT4-CT97-2183 Project "MESTRAL" (2001) Artefacts and methods to establish traceability of large CMMs – final report.
[269] Staude A, Bartscher M, Ehrig K, Goebbels J, Koch M, Neuschaefer-Rube U, Nötel J (2011) Quantification of the capability of micro-CT to detect defects in castings using a new test piece and a voxel-based comparison method. NDT and E International 44/6:531-536.
[270] Stedman M (1987) Basis for comparing the performance of surface-measuring machines. Prec. Eng. 9:149.
[271] Stolfi A, De Chiffre L (2016) 3D artefact for concurrent scale calibration in Computed Tomography. CIRP Annals, 65(1):499-502.
[272] Su R, Wang Y, Coupland JM, Leach RK (2017) On tilt and curvature dependent errors and the calibration of coherence scanning interferometers. Opt. Express 25:3297-3310.
[273] Swyt D et al. (2001). Developments at NIST on Traceability in Dimensional Measurements. Proc. SPIE, 4401.
[274] Tasic T et al. (2011). Integration of a laser interferometer and a CMM into a measurement system for measuring internal dimensions. Measurement 44/2:426-433.
[275] Thalmann R et al. (2017). Versatile calibration artefact for optical micro-CMMs based on micro-spheres with engineered surface texture. Proc. MacroScale 2017, VTT MIKES Espoo, Finland, 17-19 October; doi: 10.7795/810.20180323F.
[276] Thomas M, Su R, Nikolaev N, Coupland JM, Leach RK (2019) Modelling of coherence scanning interferometry for complex surfaces based on a boundary element method. Proc. SPIE 11057:1105713.
[277] Titov A, Malinovsky I, Massone CA (2000). Gauge Block Measurements with Nanometre Uncertainty. Metrologia 37:121-130.
[278] Tran H, Emtman C, Salsbury JG, Wright W, Zwilling A (2011) Measurement comparisons between optical and mechanical edges for a silicon micromachined dimensional calibration standard. Proc. 26th ASPE annual meeting.
[279] VDI/VDE 2630 part 2.1 (2015) Computed tomography in dimensional measurement - Determination of the uncertainty of measurement and test process suitability of coordinate measurements systems with CT sensors. VDI, Dusseldorf.
[280] Wang Q, Peng Y, Wiemann A-K, Balzer F, Stein M, Steffens N, Goch G (2019) Improved gear metrology based on the calibration and compensation of rotary table error motions. CIRP Annals 68(1):511-514.
[281] Watanabe T, Fujimoto H, Nakayama K, Masuda T, Kajitani M (2003). Automatic high-precision calibration system for angle encoder (II). Proc. SPIE 5190, doi: 10.1117/12.506473.
[282] Watanabe T et al. (2005) Self-calibratable rotary encoder J. Phys: Conf. Ser.13 240.
[283] Weckenmann A, Estler T, Peggs G, McMurtry D (2004) Probing Systems in Dimensional Metrology. CIRP Annals 53(2):657-684.
[284] Weckenmann A, Jiang X, Sommer K-D, Neuschaefer-Rube U, Seewig J, Shaw L, Estler T (2009) Multisensor data fusion in dimensional metrology. CIRP Annals, 58(2):701–721.
[285] Weichert W (2016). Implementation of straightness measurements at the Nanometer Comparator. CIRP Annals, 65-1, 507-510.
[286] Whitehouse DJ, Bowen DK, Chetwynd DG, Davies ST (1988). Nano-calibration of stylus based instruments. J Phys E Sci Instrum, 21/3:46-51.
[287] Whitehouse DJ (2010) Handbook of Surface and Nanometrology. 2nd ed. CRC Press. New York.
[288] Widdershoven I, Donker RL, Spaan HAM (2011) Realization and calibration of the 'Isara 400' ultra-precision CMM. J. Phys.: Conf. Ser. 311:012002.
[289] Wilhelm R.G., Hocken R., Schwenke H., 2001, Task specific uncertainty in coordinate measurement. CIRP Annals, 50/2, 553-563.
[290] Wilm J, Madruga DG, Jensen JN, Gregersen SS, Brix ME, Guerra MG, et al. (2018). Effects of subsurface scattering on the accuracy of optical 3D measurements using miniature polymer step gauges. Proc. euspen Venice, Italy, p. 449–450.
[291] Wu W-T et al. (2010). Method for gauge block measurement with the heterodyne central fringe identification technique. Appl. Opt. 49, 3182–6.
[292] Yagüe JA, et al. (2009) A new out-of-machine calibration technique for passive contact analog probes. Measurement, 42/3:346–357.
[293] Yandayan T (2017). Recent developments in nanoradian-angle metrology. Proc. SPIE 10385:1038509, doi: 10.1117/12.2274192.
[294] Ye J, Takac M, Berglund CN, Owen G, Pease RF (1997). An exact algorithm for self-calibration of two-dimensional precision metrology stages. Prec. Eng. 20-1:16-32.
[295] Zanini F, Carmignato S (2017) Two-spheres method for evaluating the metrological structural resolution in dimensional computed tomography. Meas. Sci. Technol. 28(11):114002.
[296] Zanini F, Carmignato S (2018) X-ray computed tomography for measurement of additively manufactured metal threaded parts. Proc. ASPE and euspen Summer Topical Meeting: Advancing Precision in Additive Manufacturing; pp. 217-221.
[297] Zanini F, Pagani L, Savio E, Carmignato S (2019) Characterisation of additively manufactured metal surfaces by means of X-ray computed tomography and generalised surface texture parameters. CIRP Annals, 68(1):515-518.
[298] Zelený V, Linkeová I, Skalník P (2015). Calibration of freeform standard, Proc. euspen; Leuven, Belgium, 1-5 June.